MODIS Level 1B Algorithm Theoretical Basis Document (Collection 7)

MODIS Characterization Support Team

Xiaoxiong Xiong, Amit Angal, Tiejun Chang, Xu Geng, Kevin Twedt, Aisheng Wu, Emily Aldoretta, Truman Wilson, Carlos Perez Diaz, Ashish Shrestha, Qiaozhen Mu

Version 1

February 21, 2025

Prepared For:
National Aeronautics and Space Administration

Table of Contents

Contents

Acknowledgement: All the present and past members of MCST are acknowledged for their efforts towards the algorithm development, testing, and implementation of the Collection 7 Level 1B.

1. INTRODUCTION

1.1. Overview

The MODerate-resolution Imaging Spectroradiometer (MODIS) is a key instrument for the NASA's Earth Observing System (EOS). The EOS was designed to provide global observations and scientific understanding of land cover changes and global productivity, sea surface temperature, atmospheric and climate changes, and natural hazards [Xiong et al., 2009].

MODIS [Xiong et al., 2005a] is a passive imaging spectroradiometer with 490 detectors, arranged in 36 spectral bands that are sampled across the visible and infrared spectrum. It is a high signal-to-noise instrument designed to satisfy a diverse set of oceanographic, terrestrial, and atmospheric science observational needs. The near-daily global coverage of MODIS, combined with its continuous operation, broad spectral coverage, and relatively high spatial resolution, makes the MODIS instruments central to the objectives of NASA's EOS program. MODIS observations and science data products are applied to many of the areas identified as EOS science topics, such as land surface composition, land surface biological activity, surface temperature, snow and sea-ice extent and character, ocean and lake physics and biogeochemical activity, aerosol properties, and cloud properties. The MODIS Proto-Flight Model (PFM) was launched December 18, 1999, on-board the Terra spacecraft in a 10:30 AM (local time, descending node) orbit. The Aqua Flight Model (FM-1) was launched onboard the Aqua spacecraft into a 1:30 PM (local time, ascending node) orbit on May 4, 2002.

The MODIS development was managed by NASA's Goddard Space Flight Center (GSFC) in Greenbelt, Maryland. The MODIS instruments were designed, built, and tested by Raytheon / Santa Barbara Remote Sensing (SBRS) in Goleta, California. The MODIS Characterization Support Team (MCST), working under the direction of the MODIS Team Leader, is responsible for the characterization and radiometric calibration of the MODIS instruments [Xiong et al., 2006]. MCST developed the Level 1B (L1B) software that converts instrument response in digital numbers (DN) to calibrated, geo-located top of the atmosphere (TOA) radiances for all bands and Earth reflectance factors for the 20 reflective solar bands (RSB). The MODIS data products provided by the MODIS Science Team support the Earth science community at large, interdisciplinary investigators, and the MODIS Science Team members' own investigations.

1.2. Historical Perspective

The MODIS was designed to continue global monitoring similar to the observations initiated with the Nimbus 7 Coastal Zone Color Scanner (CZCS), the Advance Very High Resolution Radiometer (AVHRR), the High Resolution Infrared Spectrometer (HIRS), the Landsat Thematic Mapper (TM), and the Orbview-2 Sea-viewing Wide Field of View Sensor (SeaWiFS). The selection of MODIS spectral bands and the development of many of the MODIS science data products rely on the experiences and lessons learned from predecessor missions. This continuity allows many previously existing data records to be extended with improved coverage and quality.

New features incorporated into MODIS include a thin-cirrus cloud detection channel, low gain bands to detect surface fires, and high gain bands for ocean chlorophyll fluorescence-line height discrimination. Additional information about the MODIS instrument development, MODIS requirements, and program development is presented by Barnes et al [2003]. Key MODIS specifications and design parameters are listed in Appendix A.

1.3. Document Context and Scope

This ATBD describes how MODIS operates in space and provides the equations implemented by the L1B software to generate the MODIS MOD02 (Terra) and MYD02 (Aqua) data products. It is a summary document that presents the formulae and error budgets used to transform MODIS DN to radiance and reflectance. It describes the current (Collection 7 or C7), post-launch MODIS calibration process and supersedes previous ATBDs [Barker et al. (Version 1), 1994] [MCST (Version 2), May 1997] [MCST (Version 3), December 14, 2005] [MCST (Version 4), June 14, 2013]. Analysis of instrumental on-orbit performance by MCST and investigation of L1B products by the Science Team have resulted in several L1B software updates and improvements. This ATBD corresponds to the Version 7.0 Terra and Aqua software releases. Prior to 2006, the MCST and the Science Data Support Team (SDST) provided software deliveries to the Goddard Distributed Archive and Analysis Center (GDAAC). Subsequently, the MODIS Adaptive Processing System (MODAPS) assumed the data production role formerly undertaken by the GDAAC. Product files are currently distributed using the Level 1 and Atmosphere and Archive Distribution System available at https://ladsweb.modaps.eosdis.nasa.gov.

The MODIS calibrated data product results from the application of the formulae and the determination of corresponding uncertainties described in this document and the referenced support documents. The support documents present details of how the instrument data are transformed from digital counts to (1) reflectance factors and radiances for the reflective solar bands and (2) radiances for the thermal emissive bands. Items (1) and (2) are the focus of this document and of the on-line production processing efforts. Changes in the center wavelengths for the solar reflecting bands and relative spatial shifts for the pixels along scan and the bands along track are evaluated off-line by the MCST.

The instrument is described in section 2 of this document. The key calibration equations applied by the L1B algorithms to the thermal emissive band (TEB) and the reflective solar band (RSB) data are presented in sections 3 and 4, respectively. These sections also describe MODIS instrumental effects handled within L1B and discuss the associated uncertainties in Terra/MODIS and Aqua/MODIS processing. An overview of the L1B calibration algorithm is given in section 5 and a summary follows in section 6.

1.4. Relevant Documents

Documents containing more complete derivations and explanations of the implementation of these algorithms include [EOS, 1994], [MCST (1997)], [Guenther et al., 1996], [Isaacman et al., 2003] and [Toller et al., 2008 and 2013]. Pre-launch sensor characterization publications include [GSFC, 1993], [SBRS, 1993], [SBRS, 1994], [Guenther et al., 1995], and [Barnes et al., 1998].

The L1B approach to calibration is described in the MODIS Level 1B In-Granule Calibration Code (MOD_PR02) High-Level Design [MCST, 2012a]. Program file specifications and metadata are described in the MODIS Level 1B Product Data Dictionary [MCST, 2012b]. The product format and the scaling algorithms used to generate the calibrated products are presented in the MODIS Level 1B Product User's Guide [MCST, 2012c]. The MCST web site [MCST Home Page, 2025] contains abundant Terra MODIS and Aqua MODIS mission information.

Data flow diagrams for the reflective solar and thermal emissive band algorithms, L1B input files, data products, and a discussion of the look-up tables (LUTs) that provide the parameters needed to generate L1B are summarized in Isaacman, et al., 2003. Detailed LUT documentation is also available from the MODIS LUT Information Guide [MCST, 2012d]. Solar and lunar position vectors together with the MODIS geolocation product are used within the L1B algorithm. A separate ATBD exists for the MODIS geolocation algorithms [Nishihama et al., 1997].

2. INSTRUMENT DESCRIPTION

2.1. Overview

MODIS is a passive cross-track-scanning imaging radiometer designed to take measurements in spectral regions that have been included in several heritage sensors. MODIS uses a two-sided beryllium paddle-wheel scan mirror that continuously rotates at 20.3 rpm (a scan period of 1.478s per mirror side). The instrument field of view (FOV) is ±55° from the nadir. Viewing the Earth from a sun-synchronous near polar orbit at an altitude of 705km, the two sides of the scan mirror alternately produce a swath of 2330km along scan by 10km (at nadir) along track. Both Terra and Aqua MODIS can provide near-global coverage in 2 days, enabling comprehensive short- and long-term studies of the Earth’s land, oceans, and atmosphere.

MODIS [Xiong et al., 2005a] has 36 spectral bands with wavelengths from 0.41 to 14.5 μm. The center wavelength and band-pass of each band were carefully selected to optimize measurements of key features of the Earth’s land, ocean, and atmosphere. MODIS bands 1-19 and 26 are the reflective solar bands (RSB) that provide images from daylight reflected solar radiation and bands 20-25, and 27-36 are the thermal emissive bands (TEB) that provide day and night images of thermal emissions. The measured characteristics in Table 1 can be compared to the MODIS design specifications provided in Appendix A.

MODIS bands 1-2 have a nominal nadir resolution of 250 m with 40 detectors per band along-track, bands 3-7 have a nadir resolution of 500 m with 20 detectors per band along-track, and bands 8-36 have a nadir resolution of 1 km with 10 detectors per band along-track. Bands 13 and 14 have 2 arrays of 10 along-track detectors each, providing observations with high gain and low gain through time delay and integration (TDI). Each sample for bands 13 and 14 combines the responses from a pair of TDI detectors with their signals amplified through both high and low gain amplifiers. Therefore, MODIS has a total of 490 detectors. For a 1 km (along scan) by 10 km (along track) frame of data, each detector of the 250 m resolution bands (1-2) takes 4 samples and each detector of the 500 m resolution bands (3-7) takes 2 samples. Thus, there are a total of 830 samples for each frame. MODIS digitizes each sample to 12-bit resolution. The average data rate over an orbit is 6.1 megabits per second.

Table 1: MODIS measured characteristics. Note: The Terra SNR and NEdT are for the initial on-orbit operational configuration. Terra A1 denotes the first period when Terra operated using electronics side A.

RSB BAND	Central λ Terra, Aqua nm	Bandwidth Terra, Aqua nm	Terra SNR at Ltyp	Aqua SNR at Ltyp
1	646.3, 645.8	47.8, 47.2	186	193
2	856,5, 856.9	37.7, 37.8	517	508
3	465.7, 466.1	18.6, 18.8	328	317
4	553.7, 553.9	19.7, 19.6	330	319
5	1242.3, 1241.5	23.5, 22.8	161	149
6	1629.4, 1628.1	28.4, 26.9	472	424
7	2114.2, 2113.9	52.4, 52.3	147	152
8	411.8, 412.4	14.7, 14.3	1097	1071
9	442.1, 442.2	9.6, 9.6	1495	1400
10	487.0, 487.4	10.5, 10.6	1521	1311
11	529.7, 530.1	11.9, 11.9	1604	1341
12	546.9, 547.2	10.2, 10.3	1452	1172
13	665.6, 666.0	10.0, 10.0	1413	1165
14	677.0, 677.6	11.3, 11.2	1518	1271
15	746.6, 746.8	9.9, 9.8	1519	1138
16	866.3, 866.9	15.5 ,15.5	1400	1062
17	904.2, 904.4	34.7, 34.6	379	373
18	935.7, 936.4	13.5, 13.5	76	91
19	936.2, 936.3	45.7, 46.1	509	503
26	1382.3, 1382.3	34.6, 36.4	230	282
TEB BAND	Central λ Terra, Aqua nm	Bandwidth Terra, Aqua nm	Terra NEdT (K) (Terra A1)	Aqua NEdT (K) (Aqua B)
20	3788.3, 3780.2	187.5, 186.9	0.03	0.02

21	3992.2,3981.8	82.8, 83.3	0.15	0.21
22	3972.0, 3972.0	86.1, 85.4	0.02	0.02
23	4056.7, 4061.6	85.6, 85.3	0.02	0.02
24	4473.2, 4448.3	90.2, 92.2	0.13	0.11
25	4545.4, 4526.3	91.1, 90.4	0.05	0.04
27	6770.5, 6786.8	239.1, 187.9	0.10	0.10
28	7342.9, 7349.3	320.6, 314.9	0.05	0.05
29	8528.7, 8555.3	344.1, 359.2	0.02	0.02
30	9734.1, 9723.7	297.2, 301.1	0.11	0.07
31	11018.9, 11026.2	516.3, 531.1	0.03	0.02
32	12032.1, 12042.3	520.7, 521.5	0.04	0.03
33	13365.0, 13364.7	307.6, 310.9	0.13	0.08
34	13683.3, 13685.9	324.1, 341.7	0.23	0.12
35	13913.2, 13925.2	327.7, 332.7	0.23	0.15
36	14195.6, 14215.2	284.9, 327.9	0.43	0.23

Figure 1 shows the MODIS scan cavity and the on-board calibrators. The on-board calibrators (OBCs) include a solar diffuser (SD) and solar diffuser stability monitor (SDSM), a blackbody (BB) and a space view (SV) port, and a spectro-radiometric calibration assembly (SRCA).

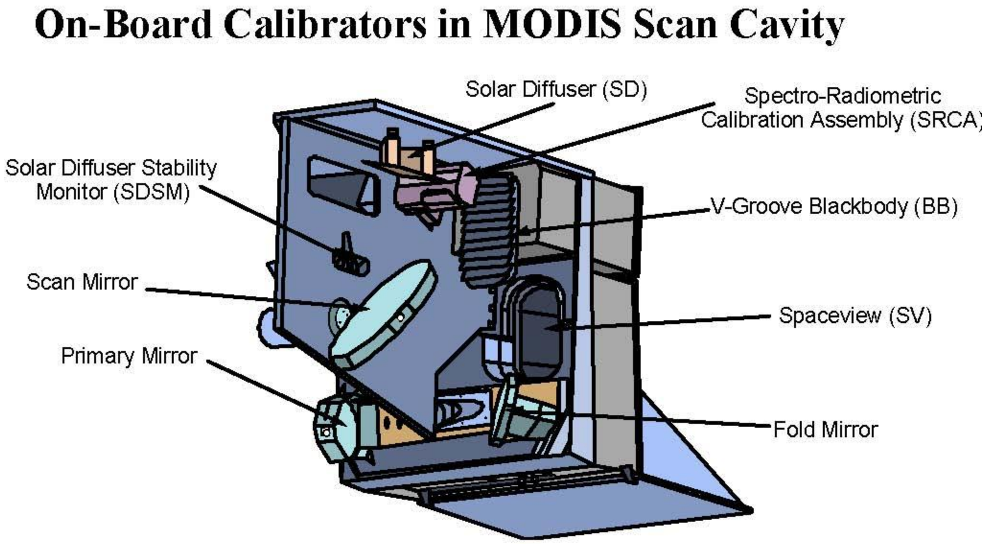
On-Board Calibrators in MODIS Scan Cavity

Figure 1: MODIS scan cavity and on-board calibrators

The optical system schematic is shown in Figure 2. The scan mirror reflects energy to the fold mirror. The aft optics consist of a two mirror off-axis telescope, and a series of dichroic beam splitters and band pass filters that separate the radiation onto four focal plane assemblies (FPAs). These are designated, according to their spectral regions, as: visible (VIS), near infrared (NIR), short and middle wave infrared (SMIR), and long wave infrared (LWIR).

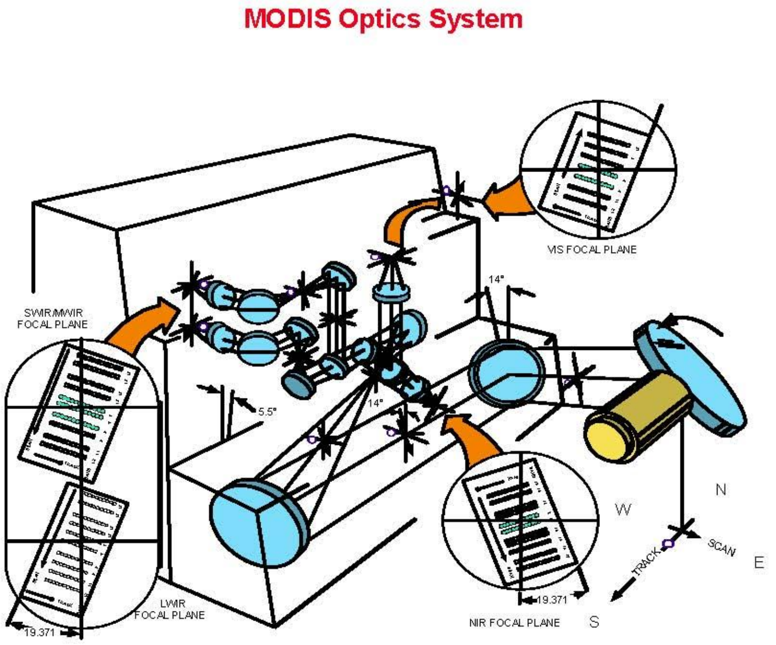

Figure 2: Schematic of the optical system

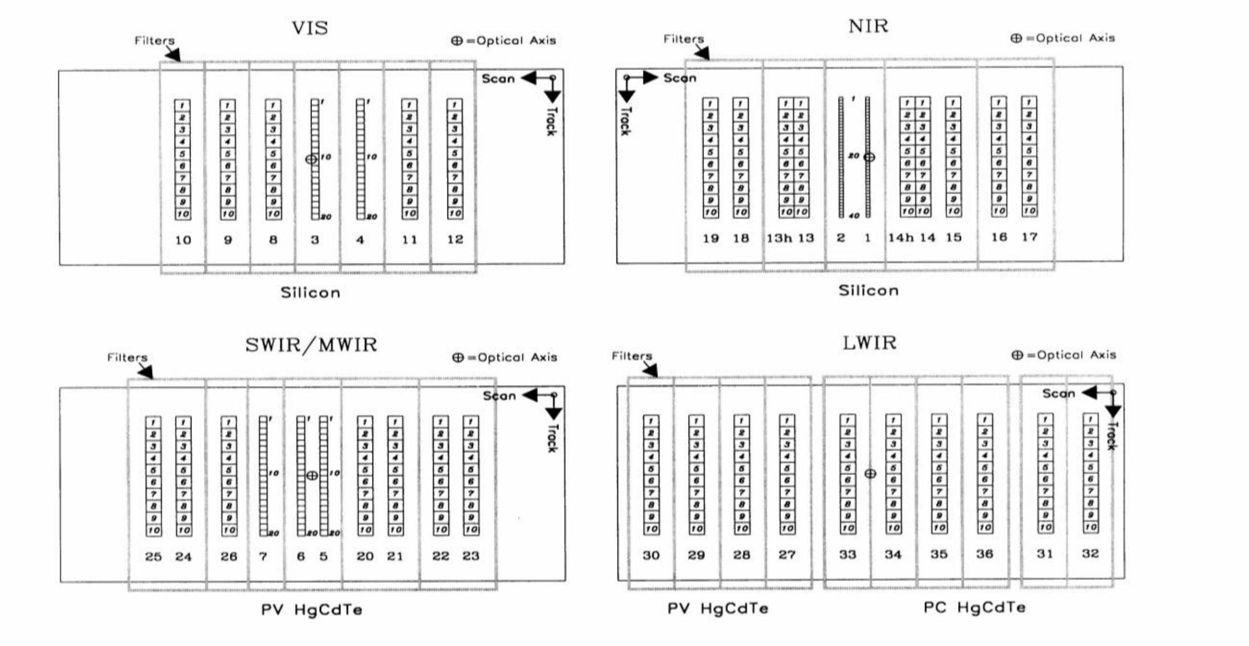

Figure 3: MODIS' focal plane assemblies

The locations of the MODIS' 36 spectral bands (490 detectors) on the four FPAs are shown in Figure 3. The detector numbering convention in Figure 3 corresponds to that of the MCST Level

1B processing and is called “product order”. Product order is the inverse of the instrument builder’s “SBRS order” detector numbering convention. The SMIR and LWIR FPA are controlled by a radiative cooler to 83 K during on-orbit operation.

The MODIS detectors view the on-board calibrators through the same optical path as the Earth observations, but at different viewing angles or at different angles of incidence (AOIs) to the scan mirror. As the MODIS scan mirror rotates, each side scans the Solar Diffuser (SD), the Spectro-Radiometric Calibration Assembly (SRCA), the Blackbody (BB), the space view (SV), and the Earth (EV). Figures 4a and 4b illustrate the scan angles and their corresponding AOIs. MODIS calibration corrects for a response versus scan angle (RVS) effect.

The VIS and NIR detector arrays are photovoltaic (PV) silicon hybrids that are operated at instrument ambient temperature. The SMIR FPA uses PV HgCdTe hybrid arrays. The LWIR FPA consists of PV HgCdTe detector arrays for bands with wavelengths less than 10 μm and photoconductive (PC) HgCdTe detectors for bands beyond 10 μm.

The analog output signals produced by the PV FPAs are buffered and digitized in the space view analog module (SAM). The signals produced by the PC detectors on the LWIR FPA are pre-amplified by the cooler located amplifier module (CLAM) and then post-amplified and digitized by the forward viewing analog module (FAM). The digital outputs from the SAM and FAM are formatted into science data packets by a formatter/processor in the main electronics module (MEM). They are then buffered and sent to the spacecraft through a first-in first-out (FIFO) buffer and fiber distributed data interface (FDDI) circuits.

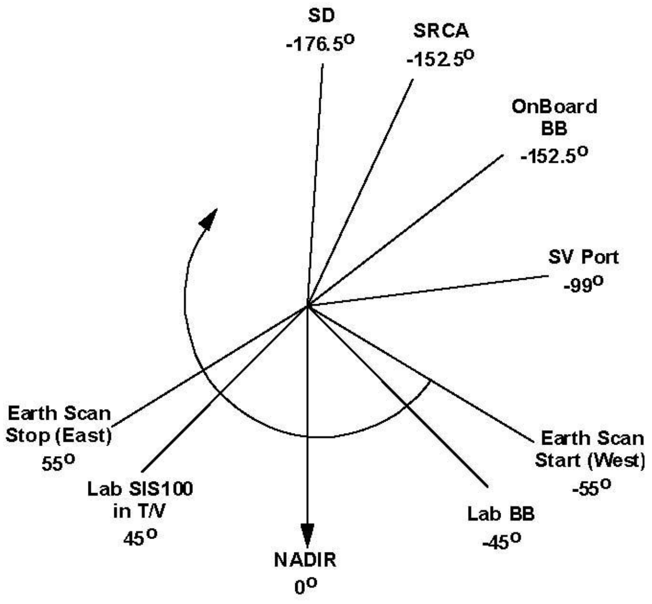

Figure 4a: The primary mirror scan angles of the ground calibration sources, space, and Earth.

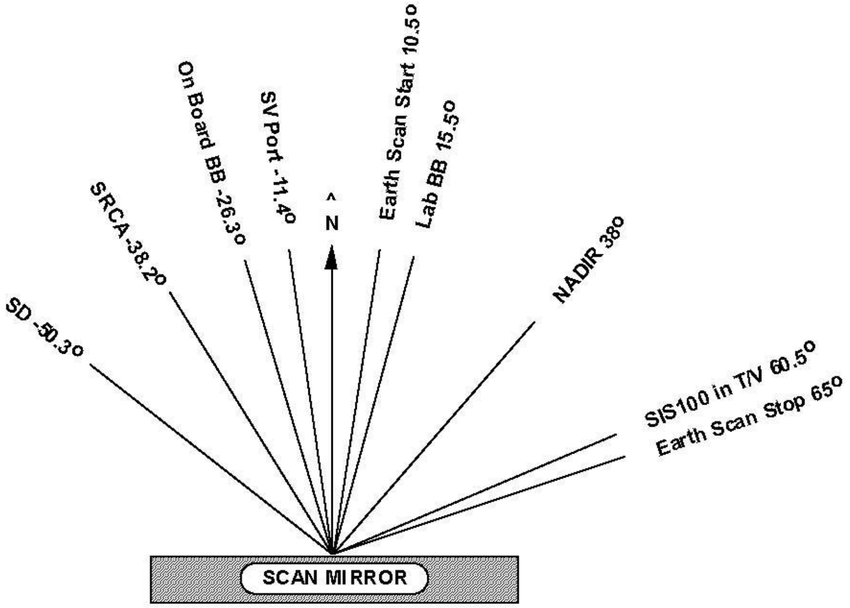

Figure 4b: The angles of incidence (AOIs) corresponding to primary mirror scan angles for the observed elements.

2.2. Solar Diffuser (SD) and Solar Diffuser Stability Monitor (SDSM)

The SD and SDSM shown in Figures 5 and 6 operate together as a system for calibrating the reflective solar bands (RSB) with wavelengths from 0.41 to 2.2 μm. The diffuser is made of space-grade Spectralon™, a proprietary thermoplastic formulation of polytetrafluoroethylene (PTFE). The SD bi-directional reflectance factor (BRF) was characterized pre-launch with National Institute of Standards and Technology (NIST) traceable reflectance standards. The SD on-orbit degradation is tracked by the SDSM during each periodic (initially weekly, currently every 3 weeks) calibration sequence. The SDSM itself is a ratioing radiometer which monitors on-orbit SD BRF variation (degradation) by alternatively viewing diffusely reflected Sun light from the SD panel and direct Sun light through an attenuation screen with a nominal 1.44% transmission. The screen is used to keep the signals from the SD and sun view at nearly the same level. The SDSM has nine filtered detectors embedded in a small solar integrating sphere (SIS) that monitors the SD degradation in the wavelength range from 0.41 to 0.94 μm. The specified MODIS RSB uncertainties are ± 2% reflectance and ± 5% absolute radiance. The reflectance calibration of the RSB from the SD measurements can be converted to a radiance calibration based on published values for the solar spectral irradiance. Two illumination levels of SD calibration are provided via a deployable 8.5% transmission screen. The screen must be in place for calibrating the high gain bands (B8-16 for ocean color observations) since they saturate when viewing direct sun exposure of the SD.

Figure 5: MODIS Solar Diffuser

Figure 6: Solar Diffuser Stability Monitor

2.3. On-board Blackbody (BB)

The thermal emissive bands (TEB) are calibrated by viewing the on-board blackbody (BB) which provides a known radiance source, and, subsequently, cold space through the Space View (SV) port providing measures of the instrument thermal background and electronic offset. This calibration is performed on a scan-by-scan basis. The on-board blackbody, shown in Figure 7, is a “V-groove” device with known emissivity (approximately 0.992) determined from pre-launch radiometric calibration and characterization. Twelve thermistors embedded beneath the BB front surface measure the temperature of the BB each scan. The thermistors were calibrated pre-launch using NIST temperature standards. The BB temperature can be varied from the MODIS scan cavity ambient of about 270 K up to 315 K by means of electrical heating elements attached to the back of the BB. This allows on-orbit checks of the TEB detectors’ non-linearity. The readings from the BB at any temperature in its operating range are also used by the instrument to adjust the detectors’ DC restore (DCR) in each scan so that an appropriate dynamic range for the electronic readout can be maintained.

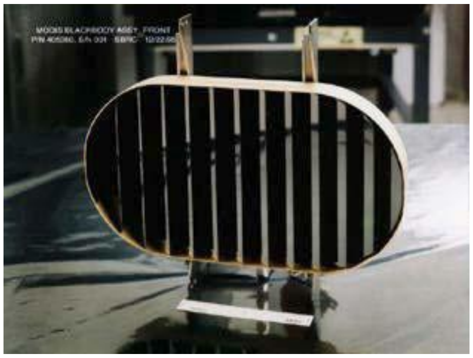

Figure 7: On-Board Blackbody Calibration Source

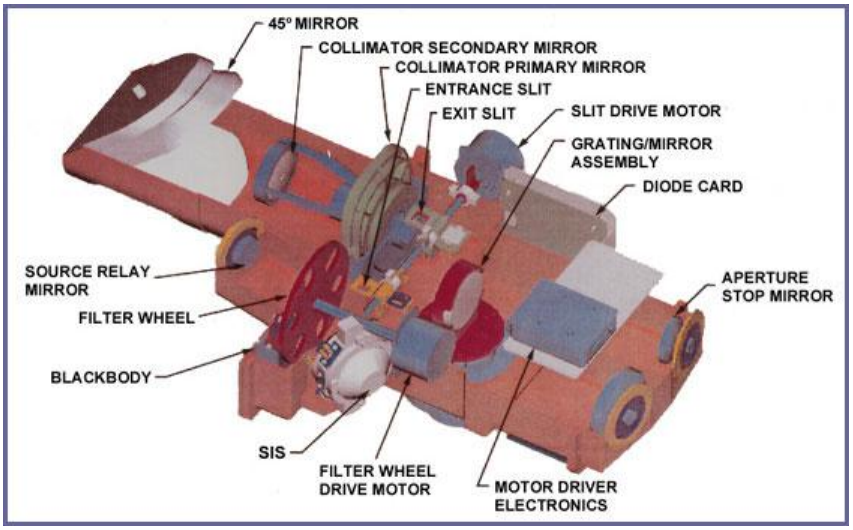

Figure 8: Spectro-Radiometric Calibration Assembly

2.4. Spectro-radiometric Calibration Assembly (SRCA)

The Spectro-radiometric Calibration Assembly (SRCA) is depicted in Figure 8. It is primarily used for spatial (all 36 bands) and spectral (RSB only) characterization. It also monitors radiometric response changes (RSB only) on-orbit. This device consists of a modified Czerny-Turner monochromator that includes a motor-driven grating/mirror assembly, a filter wheel assembly, incandescent sources, including a SIS with four 10 W and two 1 W lamps and a separate IR source, and collimating optics located at the exit slit of the monochromator. In spectral mode the SRCA is a monochromator while in spatial modes it becomes a transfer optic by replacing the grating with a plain mirror [Young, 1995a]. The SRCA spectral radiance is self-calibrated on-orbit using known and pre-launch calibrated spectral peaks in a didymium glass filter located at the exit slit of the monochrometer. In the spatial registration mode, the entrance port of the monochromator is open, and the exit slit of the monochromator is replaced with specially designed spatial reticles, one for along scan and another for along track [Young, 1995b]. The images of the reticles are projected onto the MODIS FPAs to provide instrument spatial registration information.

3. CALIBRATION ALGORITHM FOR THE THERMAL EMISSIVE BANDS (TEB)

3.1 Pre-launch Characterization and Calibration (TEB)

Each of the MODIS instruments went through a series of pre-launch comprehensive, system-level, spatial, spectral, and radiometric calibrations and characterizations. The TEB radiometric calibration was performed in a thermal vacuum (TV) environment. To cover the anticipated range of on-orbit operational conditions, three different temperature plateaus (nominal, cold, and hot) were used during instrument characterization and performance evaluation. Both primary and redundant electronics configurations were tested during radiometric calibration. In addition, different cold focal plane assembly (CFPA) temperature set points were used to characterize the TEB detectors' response changes and sensitivity. The key pre-launch equipment used for the TEB calibration is a large-aperture variable-temperature blackbody calibration source (BCS) with an emissivity better than 0.9995 over the TEB spectral range. A photograph of the BCS is shown in Figure 9. A space view source (SVS), like the BCS, operated at an extremely low fixed temperature was used to simulate the deep space view. MODIS TEB pre-launch calibration and characterization included deriving and evaluating each detector's gain (or linear response), non-linearity, noise characteristics, and short-term stability. Some of the parameters obtained pre-launch are also used for the instrument's on-orbit calibration and radiometric uncertainty assessment.

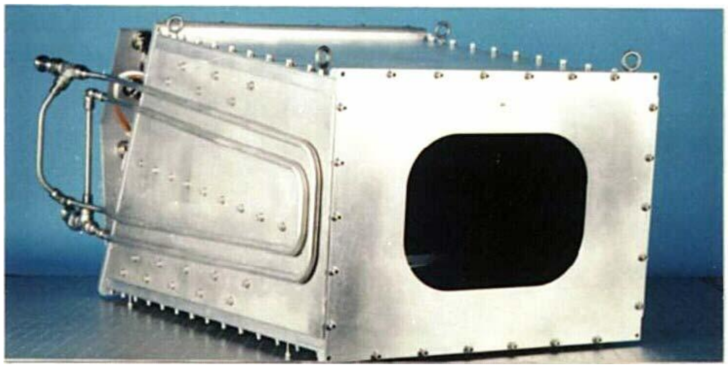

Figure 9: Blackbody Calibration Source (BCS)

The temperature of the on-board BB, shown in Figure 7, was set at 290K (Terra) and 285K (Aqua) during most of the calibration tests while the BCS temperature was varied from 170K to 340K. These tests were performed under several different operational conditions including different instrument temperatures and different CFPA temperatures. Determination of the on-board BB emissivity is one of the most important tasks to be completed in order to assure a high-quality pre-launch to on-orbit radiometric calibration transfer. The BB emissivity for each thermal emissive band is determined from the detectors' responses to the BCS and the BB at the same time.

The MODIS TEB calibration algorithm is based on a quadratic relationship between the detector's response and the input radiance [Goldberg, 1995]. The offset and nonlinear terms derived from the pre-launch radiometric calibration are also used for the initial on-orbit calibration. They are updated on-orbit as needed. There are several improvements in the MODIS FM1 design, and its pre-launch TV radiometric calibration test procedure based on lessons learned from the PFM TV tests. Both instruments were modified after TV system level tests. The changes were made prior to launch, either to correct identified problems or to improve the sensors' performance using the pre-launch calibration and characterization data. Because of these changes, additional post launch efforts were required to assure on-orbit calibration and characterization quality.

MODIS uses a double-sided scan mirror to make observations of the Earth scenes in a ±55° scan angle range about the nadir. For each mirror side, this (scan angle) range corresponds to 1354 EV frames of data with angles of incidence (AOI) on the scan mirror ranging from 10.5° to 65.5° (see Figure 4b). Since the sensor response changes with scan mirror AOI whereas the calibration is performed at a single AOI, it is essential to accurately characterize the sensor's response versus scan-angle (RVS). For the Terra MODIS (PFM), there are no valid pre-launch RVS measurements for the TEB. Initially, the Terra MODIS TEB RVS values were derived using scan mirror witness-sample reflectance measurements (by the National Physical Lab, Great Britain) and the coupling parameters derived from the Aqua MODIS (FM1) TEB RVS measurements. Currently, the Terra MODIS thermal emissive bands use the RVS values derived from on-orbit deep space maneuvers [Xiong et al 2005a].

3.2 On-orbit Calibration Algorithm (TEB)

The MODIS TEB on-orbit calibration is performed for each band, detector, and mirror side during nominal operations [Xiong, et al., 2002a]. During MODIS on-orbit nominal operation, the blackbody temperature is controlled at a stable temperature: 290K for Terra for most of the mission and 285K after April 2020, and 285K for Aqua for the entire mission. The BB temperature setting for each instrument corresponds to the BB temperature at which most of the pre-launch calibration and characterizations were performed in the thermal vacuum environment. Calibration is scan angle dependent and is performed on a scan-by-scan basis. During each scan, the sensor views the on-board calibrator (OBC) blackbody (BB) at a known temperature (or radiance) and deep space through the instrument space view (SV) port to measure the instrument's thermal background and electronic offset. The calibration coefficients determined are then used for the Earth view (EV) scene radiance retrieval. There are 50 frames (samples) of data collected in each scan when viewing both the BB and SV sectors. The instrument response is provided in 12-bit digital numbers (DN). When the sensor views the BB via its scan mirror, the total path radiance includes the radiance from the BB emission (L_{BB}), the radiance due to the scan mirror emission (L_{SM}), the scan cavity emission (L_{CAV}) reflected from the BB, and the thermal background (L_{BKG}). Thus, the BB view path radiance (L_{BB_path}) is

$$L_{BB\_path} = RVS_{BB} \cdot \varepsilon_{BB} \cdot L_{BB} + (1 - RVS_{BB}) \cdot L_{SM} + RVS_{BB} \cdot (1 - \varepsilon_{BB}) \cdot \varepsilon_{CAV} \cdot L_{CAV} + L_{BKG} \tag{3.1}$$

where

L_{BB_path} is the BB view path radiance.
RVS_{BB} is the normalized system response versus scan angle when the sensor views the BB.

ε_{BB} is the emissivity of the BB.
ε_{CAV} is the emissivity of the scan cavity.
L_{BB} is the radiance from the BB emission.
L_{SM} is the radiance from the scan mirror emission.
L_{CAV} is the radiance of the scan cavity reflected from the BB.
L_{BKG} is the radiance from the thermal background.

The RVS for each band and mirror side was determined pre-launch and normalized to the value at the BB view. The term (1-RVS_{BB}) is equivalent to the emissivity of the scan mirror at the BB view angle. This term, in general, varies with the scan angle or the angle of incidence (AOI) to the scan mirror. The cavity contribution is reflected from the BB with a reflectivity of (1-ε_{BB}). This term becomes smaller with higher BB emissivity. For simplicity, we do not specify the mirror side, the spectral band, and the detector indices throughout this algorithm derivation.

Similarly, when the sensor views deep space ("zero" radiance) through the SV port, the total path radiance can be expressed as,

$$L_{SV\_path} = (1 - RVS_{SV}) \cdot L_{SM} + L_{BKG} \tag{3.2}$$

where

L_{SV_path} is the SV view path radiance.
RVS_{SV} is the normalized system response versus scan angle when the sensor views deep space. L_{SV_path} includes only a scan mirror term and the background term. Note that the scan mirror terms in equation 3.1 and equation 3.2 are not the same since the RVS is a function of the AOI to the scan mirror. The path radiance difference between equations 3.1 and 3.2 is related to the sensor's response difference between the EV and SV given by;

$$dn_{BB} = \langle DN_{BB} \rangle - \langle DN_{SV} \rangle \tag{3.3}$$

where $\langle DN_{BB} \rangle$ and $\langle DN_{SV} \rangle$ represent the frame average of the sensor's BB and SV digital response during each scan.

During the BB warm-up and cold-down (WUCD) cycles, the BB temperature varies from instrument ambient temperature (~270K) to 315K. This process starts with an initial cool-down from BB nominal operating temperature to the instrument ambient. During the warm-up process, a few intermediate temperature plateaus between instrument ambient and 315K are added, allowing TEB detectors' noise characterization to be performed at different radiance or temperature levels. Once the BB temperature has reached 315K, a complete and continuous cool-down process is followed. Finally, the BB temperature is brought back to its nominal setting.

Using WUCD data, a quadratic fit of BB path radiance difference vs. response difference (dn_{BB})

is written as,

$$RVS_{BB} \cdot \epsilon_{BB} \cdot L_{BB} + (RVS_{SV} - RVS_{BB}) \cdot L_{SM} + RVS_{BB} \cdot (1 - \varepsilon_{BB}) \cdot \epsilon_{CAV} \cdot L_{CAV} = a_0 + b_1 \cdot dn_{BB} + a_2 \cdot dn_{BB}^2 \tag{3.4}$$

where, a_0, b_1, and a_2 are the quadratic polynomial coefficients. Note that we purposely use b_1, instead of a_1 in the calibration equation to emphasize the on-orbit scan-by-scan computation of the linear coefficient from the sensor's response to the BB. The radiance term, e.g. L_{BB}, is computed using the Planck equation averaged over the detector's relative spectral response, $RSR(\lambda)$

$$L_{BB}\,(T_{BB}) = \frac{\sum RSR\,(\lambda)\cdot Planck\,(\lambda, T_{BB})}{\sum RSR\,(\lambda)} \tag{3.5}$$

where

λ is the wavelength of the emission incident to the given detector.
$RSR(\lambda)$ is the relative spectral response of the detector.
Planck symbolizes the Planck black body equation.

Similar expressions apply to L_{SM} and L_{CAV}. The temperatures of the blackbody, scan mirror, and instrument cavity are determined from the instrument's telemetry using conversion coefficients. Equation 3.4 is used to calculate the TEB calibration coefficient, b_1, which is the dominant term in this quadratic algorithm. The offset and non-linear terms account for the fitting process residues or errors and small detector non-linearities over the dynamic range. They are provided in the LUTs with values determined from pre-launch calibration and updated from on-orbit BB WUCD cycles.

Currently in the L1B algorithms (for both Terra and Aqua MODIS), the a_0 term is set to zero for B31-B36, with a few exceptions to account for mirror side differences [Chang et al., 2021]. These bands typically view scenes at temperatures (see Table 1) much lower than the BB's lowest ambient temperature of about 270K. Other parameters, such as emissivity, relative spectral response (RSR) and response versus scan-angle (RVS), determined from pre-launch calibration, are also included in the L1B LUTs.

The same quadratic algorithm approach is used for the Earth view (EV) radiance retrieval process. Using the sensor's EV and Space View (SV) response, equation 3.4 becomes

$$RVS_{EV} \cdot L_{EV} + (RVS_{SV} - RVS_{EV}) \cdot L_{SM} = a_0 + b_1 \cdot dn_{EV} + a_2 \cdot dn_{EV}^2 \tag{3.6}$$

where dn_{EV} is the sensor's EV response in digital number (DN_{EV}) with the average response to the space view ($\langle DN_{SV} \rangle$) from the same scan subtracted, that is,

$$dn_{EV} = DN_{EV} - \langle DN_{SV} \rangle \tag{3.7}$$

Once the EV radiance is retrieved, the top of the atmosphere (TOA) brightness temperature of the scene can be determined using the Planck equation.

3.3 Special Considerations in the TEB Calibration Algorithm

The TEB algorithm described above applies to both the Terra MODIS L1B and the Aqua MODIS L1B. However, there are circumstances that do not work well with the general algorithm that assumes all detectors are functional and that all bands behave similarly. In order to achieve high quality calibration for all the bands, modifications are made to deal with cases that cannot be calibrated with the general algorithm.

Keeping separate L1B code for Terra and Aqua MODIS makes it easy to address the special features in each instrument and to update the code and the LUTs for each sensor as required. Special considerations are required for the band 21 calibration (fire detection band), for the algorithm to remove Terra MODIS photo-conductive (PC) bands' optical leak, for the approach used to retain the Aqua MODIS bands 33, 35, and 36 on-orbit calibration when the blackbody temperature is above their saturation limits, and for the presence of the moon in the SV port. Most of these issues were identified from pre-launch testing and characterized prior to the instruments' launches. As the missions aged, additional corrections for electronic crosstalk have been added to the algorithms for some TEB, as well as some specialized adjustments to the non-linear coefficients to improve long-term stability. On-orbit observations continue to track the potential changes and to monitor the performance of these special algorithms or approaches.

3.3.1 Band 21 Calibration

MODIS band 21 has low gain photovoltaic (PV) detectors with a specified center wavelength at 3.96 µm, a typical scene temperature of 335K, and a maximum scene temperature of 500K. This mid-wave spectral band is used primarily for fire detection. At a typical blackbody temperature of 285K for Aqua MODIS and 290K for Terra MODIS (285K since April 2020), the sensor's response, dn_{BB}, of B21 is very small. The linear calibration coefficient, b_1, calculated from the on-board BB, fluctuates widely from scan to scan because of this low signal-to-noise ratio. Thus, the general scan-to-scan calibration method cannot provide an accurate and stable calibration for B21.

Instead of computing B21 gain on a scan-by-scan basis, a set of fixed linear coefficients is put into a LUT and used in the L1B code for B21 calibration. These linear coefficients are monitored and updated, if necessary, using on-orbit scheduled BB WUCD cycles. B21 has less stringent calibration uncertainty requirements. The offset and nonlinear terms of B21 have been set to zero in the TEB calibration algorithm. Since the MODIS TEB calibration is detector and mirror-side dependent, there are 20 coefficients for the 10 detectors and two mirror sides (L1B did not apply any mirror side difference in B21 prior to version 5). This fixed coefficient LUT approach is specifically designed for B21 and used in both Terra and Aqua MODIS calibration.

3.3.2 Terra MODIS PC Bands Optical Leak

MODIS bands 31-36 utilize photo-conductive (PC) detectors located on the LWIR CFPA. The other TEB bands use photovoltaic (PV) detectors. During pre-launch PFM instrument characterization, an optical leak (or crosstalk) from B31 to the other PC bands was identified. This problem was verified on-orbit from Earth scenes and lunar observations. Examples of Terra MODIS lunar view responses for band 31 and 33 are shown in Figure 10. The plot of band 31 response (detector 5) shows a smooth profile. The response profile of band 33 shows a small side peak that is due the optical leak from band 31 as discerned from the frame offset between the two bands. The frame offset is related spectral band location on the focal plane (see Figure 3).

To remove the optical leak from the contaminated instrument responses (dn) for these PC bands (bands 32-36) when the sensor views the BB and the EV sectors, a special correction algorithm was developed and implemented in the Terra MODIS L1B code. It is designed to make the correction by subtracting the contributions from band 31 into the other PC bands. Assume dn^{corr} is the correct response if there were no B31 optical leak, dn^{cont} is the response with the optical leak, and $xtalk_{B31 \rightarrow B}$ is the crosstalk coefficient from B31 to a given PC band. The crosstalk coefficients for each PC band are in the L1B LUT for on-board calibration and EV retrieval. The correction algorithm (using B32 as an example) is given by,

$$dn_{B32}^{corr}(F) = dn_{B32}^{cont}(F) - xtalk_{B31\ to\ B32} \cdot dn_{B31}(F + FO_{B31-B32}) \qquad (3.8)$$

where

$dn_{B32}^{cont}(F)$ is the digital response for band 32 before correction for band 31 optical leak.

$dn_{B32}^{corr}(F)$ is the digital response for band 32 after correction for band 32 optical leak

F is the data frame number.

$FO_{B31 \rightarrow B32}$ is the data frame offset between band 31 and band 32.

$xtalk_{B31 \rightarrow B32}$ is the optical leakage coefficient for band 31 into band 32.

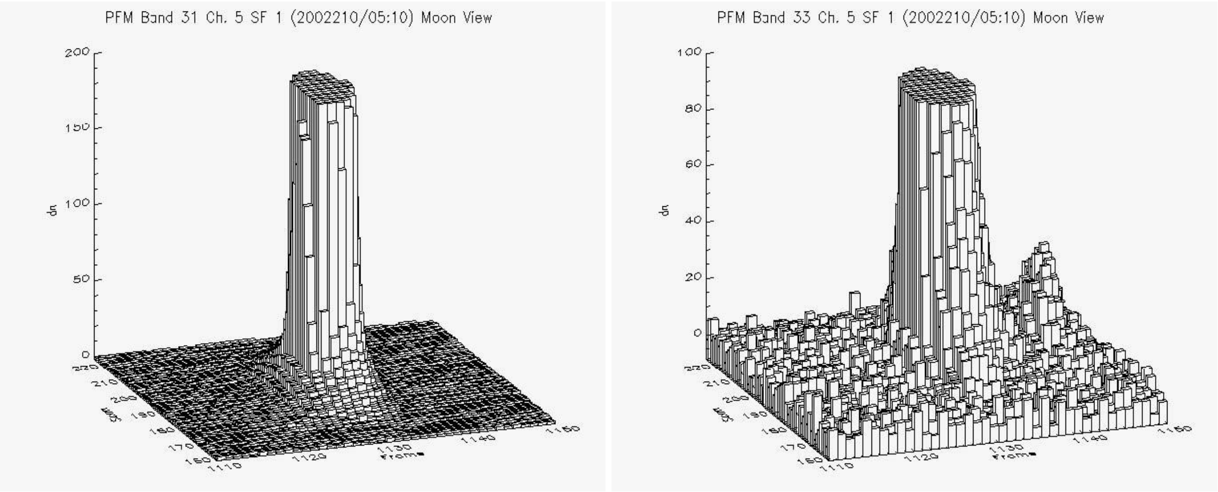

Figure 10: The Terra MODIS lunar response for B31 (left figure) and B33 (middle detectors only). The X-axis represents the data frame number, the Y-axis is the scan number, and the Z-axis is the response (dn).

This correction is applied to B32-36 on a detector-by-detector basis for both the BB calibration and the Earth scene (pixel-by-pixel) retrievals. Figure 11 shows images for band 35 with and without the PC optical leak correction. Because of the lessons learned from Terra MODIS (PFM) and subsequent improvements made in Aqua MODIS (FM1), there is no optical leak among Aqua's PC bands. Therefore, the above correction is only used in the Terra MODIS L1B calibration algorithm.

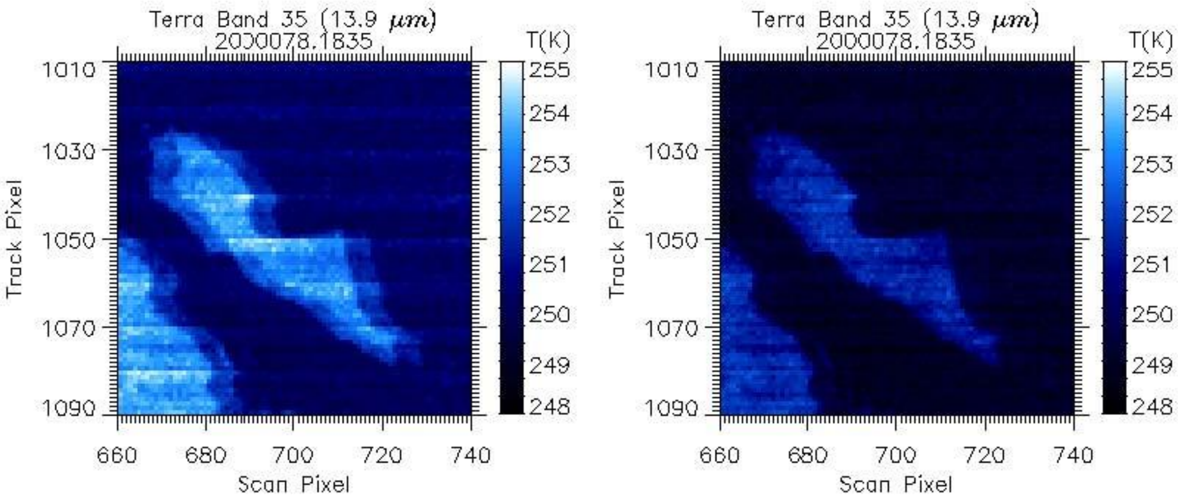

Figure 11: Band 35 Images Before and After PC Crosstalk Correction.

3.3.3 Aqua MODIS Bands 33, 35, and 36 On-orbit Calibration

On-orbit, the BB can be heated from instrument ambient to 315K. However Aqua MODIS bands 33, 35, and 36 saturate before the BB temperature reaches 315K. The saturation temperatures can vary due to instrument background and DC Restore (DCR). When the BB temperature is above the saturation limits, the scan-by-scan calibration approach of equation 3.4 can no longer be used for these three bands.

In order to keep Earth view data calibrated in this situation, a revised algorithm was developed and implemented. To account for the CFPA temperature fluctuation and to minimize the uncertainty in the estimation of the default b_1, the new algorithm calculates the CFPA temperature dependent default b_1 to calibrate these bands when $T_{BB}>T_{sat}$. The algorithm is based on the linear relationship between b_1 and the LWIR CFPA temperature for bands 33, 35, and 36. The default b_1 is calculated by

$$b_1 = b_{1baseline,\,LUT}\,[1 + c_{1LUT}\,(T_{LWIR} - T_{baseline,LUT})], \qquad (3.9)$$

where the LWIR FPA temperature T_{LWIR} is measured scan-by-scan. Other inputs to the L1B code are provided by a set of LUTs, including:

- c_1: is the rate of change of relative b_1 as a function of LWIR FPA temperature; c_1 is calculated for each BB WUCD event through the fitting of b_1 and T_{LWIR} to a set of three-orbit data prior to the BB WUCD;
- $T_{baseline}$: is a baseline LWIR FPA temperature estimate and is currently set at 83K for Bands 33, 35-36.

$b_{1baseline}$: The $b_{1baseline}$ coefficient is the supposed b_1 coefficient when the LWIR temperature is $T_{baseline}$. $b_{1baseline}$ is calculated for each BB WUCD event through the fitting of b_1 and T_{LWIR} to a set of three-orbit data prior to the BB WUCD. Three sets of LUTs are used by L1B to calculate the calibration coefficients for bands 33, 35, and 36 during the saturation periods. These LUTs are updated, when necessary, with the most recent on-orbit detector response. The saturation temperatures for these bands are in a LUT that is updated as needed based on WUCD data.

3.3.4 Moon in the SV Port

Typically, the SV signal is subtracted as in equation 4.3. However, the SV digital counts are unreliable if the Moon is in the SV port. Prior to 9/11/02 such data was flagged as unusable. Subsequently, L1B was upgraded to handle this event by including only a specified number of the dimmest frames in the calculation of the average background. A QA flag is set for the scan whenever this is done, and a metadata field reports the percentage of pixels affected.

3.3.5 Terra and Aqua LWIR crosstalk correction

The LWIR bands of MODIS (bands 27-36) use both PV and PC detectors for bands 27-30 and 31-36 respectively. The PV LWIR bands share the same sampling electronics, and throughout the Terra and Aqua missions, contamination from electronic crosstalk has been increasing among these bands, albeit to a much smaller extent for Aqua. This contamination has been shown to introduce significant radiometric biases and detector-to-detector differences in the Level-1B calibrated radiance products. It also decreases the quality of the downstream science products that rely on these bands. The contamination can be observed clearly during lunar observations, where the spatial offset of the four bands on the FPA (see Figure 3) allows us to better isolate the contaminating signal originating from each of the bands. For these bands, the contamination manifests itself as a signal that is below the background level just outside of the observed lunar signal for a given detector, as seen in Figure 12 in the case of Terra. The location of each contaminating signal allows us to identify which band and detectors are sending the contaminating signal and derive correction coefficients which can be applied to the MODIS Level-1A and OBC BB data.

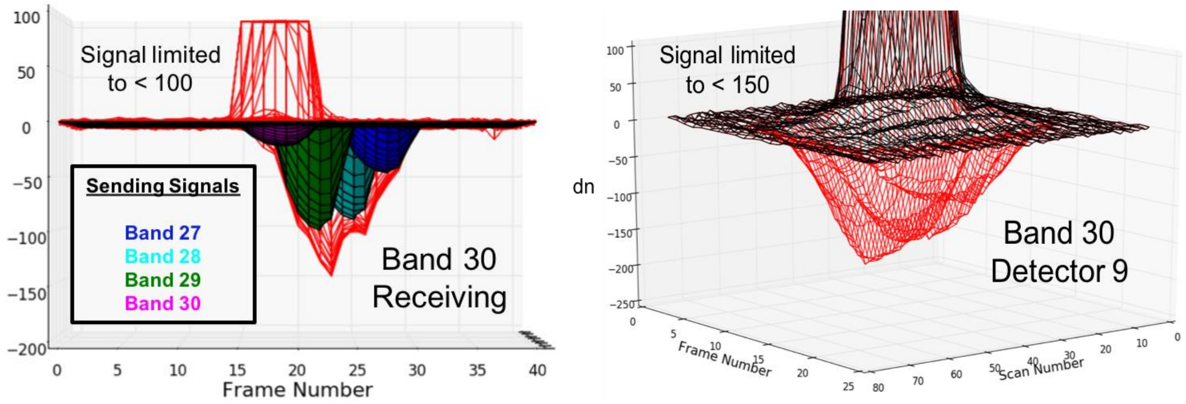

Figure 12: (left) Example of the sending signal alignment from each of the Terra PV LWIR bands with respect to the contaminated signal of band 30 detector 9 in February 2014. (right) Example of the lunar observation data for Terra band 30 detector 9 before (red) and after (black) correction in August 2015. The correction removes all the signal that is significantly below the background level.

The derived crosstalk coefficients are applied to the data from both the BB view and EV, which allows us to derive the corrected gain coefficients for each detector and to correct the EV scene data. This correction is also applied to the BB WUCD events which allow us to correct the non-linear gain coefficients as well. The coefficients are applied using the following equation:

$$dn_i(S,F) = dn_i^*(S,F) - \sum_j c_{i,j} \cdot dn_j^*(S,F + \Delta F_j)\,, \tag{3.10}$$

where dn^* is the measured (contaminated) signal after background subtraction, S/F are the scan/frame respectively, i/j are the receiving/sending detectors respectively, $c_{i,j}$ is the crosstalk coefficient matrix, and ΔF_j is the frame offset associated with the sending band with respect to the receiving band. More details on the derivation of the correction coefficients are described by Wilson et al. (2017). The crosstalk correction provides a significant improvement to the calibration coefficients and contaminated signals. As a result, Level-1B images of these bands are significantly improved, with more accurate radiometry and a reduction in the detector-to-detector striping, providing a positive impact to the MODIS Level-1B and Level 2 products throughout the mission. The Aqua band 28 crosstalk contamination is negligible early in the mission and therefore a crosstalk correction is not applied prior to 2012. For Aqua only, additional corrections are made to the Moon-derived crosstalk coefficients to reduce striping in the Earth scene images. More details on the application of the crosstalk correction for Collection 7 are described by Chang et al. (2021) and Pérez Diaz et al. (2025).

3.3.6 Terra and Aqua MWIR crosstalk correction

Similarly, to the PV LWIR bands, the MODIS PV MWIR bands share the same sampling electronics and there is electronic crosstalk contamination among them, which can clearly be seen from Moon observations. In the case of the PV MWIR bands, this contamination has been shown to introduce some radiometric biases but mostly detector-to-detector differences in the Level-1B calibrated radiance products. As an example, the signal contamination for Terra band 22 detector 8 and sending signal alignment with the contamination for band 23 detector 10 is illustrated in Figure 13. In this instance, there are several anomalous peaks that represent contamination outside of the main lunar signal from bands 20, 21, 23, 24 and 26. Likewise, the location of each contaminating signal allows us to identify which band and detectors are sending the contaminating signal and derive correction coefficients.

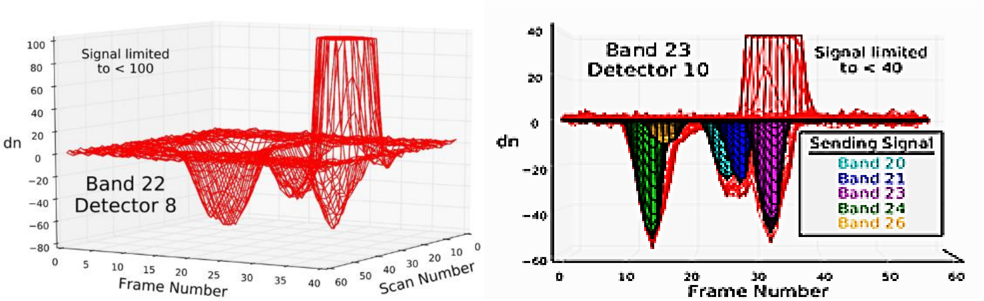

Figure 13: (left) Example of the lunar observation data for Terra band 22 detector 8 on May 2016. (right) Example of the sending signal alignment from the Terra PV MWIR bands with respect to the contaminated signal of band 23 detector 10 for the same date.

In a similar fashion to the PV LWIR bands, the derived coefficients are applied to both the BB and EV data to ultimately correct the EV scene data. The correction is also applied to the BB WUCD events to correct the MWIR non-linear calibration coefficients as well. The crosstalk coefficients are also applied using equation 3.10. The crosstalk correction provides a significant improvement to the calibration coefficients and contaminated signals. As a result, the Level-1B images of the MWIR bands are also improved. For Terra, this correction is applied to band 22 detector 8, band 23 detectors 1 and 10, and band 24 detector 1. Moreover, in the case of the band

26 detector 10 contaminated sending signal for these 4 detectors, the crosstalk correction coefficients are derived using daytime EV data over ice cloud-covered scenes. In the case of Aqua, the correction is applied to detector 1 of bands 20, 22, 23, 24, and 25. All these corrections show a significant reduction in the detector-to-detector differences and provide an overall positive impact to the MODIS Level-1B and Level 2 products. Chang et al. (2021) provides more details on the crosstalk coefficients and correction application for the MODIS MWIR bands.

3.3.7 Special corrections to the calibration coefficients

The C7 TEB calibration algorithm changes focus on the improvements on the mirror side consistency and long-term stability. The major improvements in the Terra calibration of nonlinear response function include: (1) Terra early mission PC bands a_0 correction to reduce the mirror side difference; (2) Terra bands 20 and 29 a_0 correction and a_2 re-process to decrease cold scene bias; (3) Before 2010, use of fixed a_0 and a_2 for Terra band 30 to improve its calibration stability. After 2010, the on-orbit a2 is scaled by a linear adjustment factor from 0.74 starting Jan. 2011 to 0.57 at Feb. 2016 and then time independent at 0.5 after Feb. 2016. Future adjustments after the 2025 release of C7 will be made depending on the measurement stability and calibration assessments. For Aqua MODIS TEB, the major C7 calibration algorithm changes are (1) Mission-long a_0 correction using the quasi-deep convective clouds technique (qDCC) to reduce the mirror side difference; (2) Aqua TEB a_2 update using BB CD; (3) For bands 27-30, a_0 correction from qDCC measurement drift. In addition to the calibration algorithm improvements, the C7 procedure improvements include the calibration coefficient moving average to avoid crossing the timelines of the special instrument setting changes, configuration changes, and special events such as safe mode. The LUT update frequency is increased to follow the instrument gain and performance changes, including a_0 and a_2 updates after the electronic crosstalk update and uncertainty updates for each a_0 and a_2 update. More details are provided in Chang et al. (2021) and Pérez Diaz et al. (2025).

3.4 Uncertainty (TEB)

MODIS L1B data products also include uncertainty indices (UI) that are computed for all pixels. The TEB uncertainty algorithm is based on the on-orbit calibration and scene radiance retrieval equations. It calculates the uncertainty using on-orbit observations and some input parameters determined from pre-launch calibration and characterization. The TEB calibration total uncertainty can be computed by combining the contributions from all the factors involved in the calibration and retrieval, as described by Madhavan et al. (2013). To establish an uncertainty coefficient for each term, a partial derivative with respect to each individual term is calculated [Wenny et al. (2012)].

The uncertainty components are broken down into 15 contributing factors. The total TEB uncertainty is estimated as such:

$$\frac{dL_{EV}|i}{L_{EV}} = \sqrt{\sum_i \begin{matrix} \left(\frac{dL_{EV}|a_0}{L_{EV}}\right)^2 + \left(\frac{dL_{EV}|b1_{B21}}{L_{EV}}\right)^2 + \left(\frac{dL_{EV}|a_2}{L_{EV}}\right)^2 + \left(\frac{dL_{EV}|RVS_{EV}}{L_{EV}}\right)^2 + \left(\frac{dL_{EV}|RVS_{SV}}{L_{EV}}\right)^2 \\ + \left(\frac{dL_{EV}|T_{BB}}{L_{EV}}\right)^2 + \left(\frac{dL_{EV}|T_{SM}}{L_{EV}}\right)^2 + \left(\frac{dL_{EV}|T_{CAV}}{L_{EV}}\right)^2 + \left(\frac{dL_{EV}|\lambda}{L_{EV}}\right)^2 + \left(\frac{dL_{EV}|\varepsilon_{CAV}}{L_{EV}}\right)^2 \\ + \left(\frac{dL_{EV}|\varepsilon_{BB}}{L_{EV}}\right)^2 + \left(\frac{dL_{EV}|dn_{EV}}{L_{EV}}\right)^2 + \left(\frac{dL_{EV}|dn_{BB}}{L_{EV}}\right)^2 + \left(\frac{dL_{EV}|PCX_{B32-36}}{L_{EV}}\right)^2 + \left(\frac{dL_{EV}|PVX_{B20-30}}{L_{EV}}\right)^2 \end{matrix}} \,. \qquad (3.11)$$

As mentioned in Section 3.3.6, Collection 7 introduces an electronic crosstalk correction (PVX) that is applied to the MWIR bands. A similar correction is applied to the PV LWIR bands (Sec. 3.3.5). This crosstalk correction affects the UI in the L1B product, which is a measure of the radiance uncertainty on the pixel level. In C7, an additional crosstalk uncertainty penalty is added to the total TEB uncertainty to account for any uncorrected drift in the radiance for these bands. The uncertainty penalty is calculated for every pixel throughout the mission by using the crosstalk coefficients residual between the mission-long trends and their respective linear fits with a three-year moving average. Uncertainty penalty coefficients are introduced in the same LUT format as the crosstalk coefficient LUTs, and the crosstalk coefficient uncertainty is estimated using the algorithm described by Chang et al. (2022). Table 2 shows the relationship between the UI scaling factor output in the L1B data and the percent uncertainty (radiance) for the MODIS TEB.

Table 2. L1B Uncertainty Index (UI) mapped to TEB absolute uncertainty in percent.

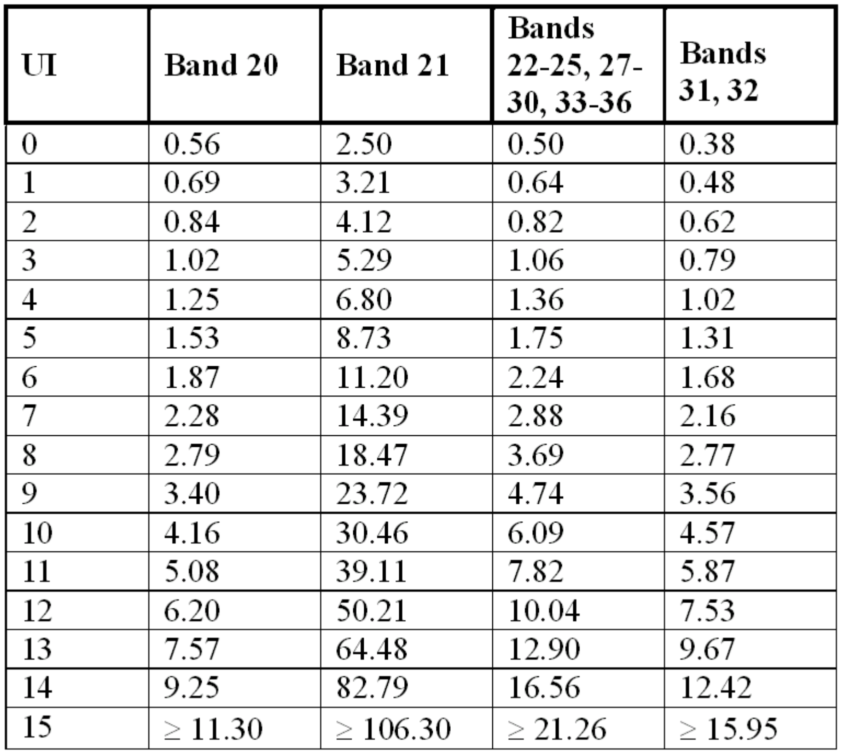

UI	Band 20	Band 21	Bands 22-25, 27-30, 33-36	Bands 31, 32
0	0.56	2.50	0.50	0.38
1	0.69	3.21	0.64	0.48
2	0.84	4.12	0.82	0.62
3	1.02	5.29	1.06	0.79
4	1.25	6.80	1.36	1.02
5	1.53	8.73	1.75	1.31
6	1.87	11.20	2.24	1.68
7	2.28	14.39	2.88	2.16
8	2.79	18.47	3.69	2.77
9	3.40	23.72	4.74	3.56
10	4.16	30.46	6.09	4.57
11	5.08	39.11	7.82	5.87
12	6.20	50.21	10.04	7.53
13	7.57	64.48	12.90	9.67
14	9.25	82.79	16.56	12.42
15	≥ 11.30	≥ 106.30	≥ 21.26	≥ 15.95

4. CALIBRATION ALGORITHM FOR THE REFLECTIVE SOLAR BANDS (RSB)

4.1 Pre-launch Characterization and Calibration (RSB)

Pre-launch, the MODIS reflective solar bands, B1-19 and 26, were calibrated using a 1-meter diameter spectral integrating source (SIS-100), shown in Figure 12. The combination of different lamps of the SIS-100 provided numerous radiance levels, allowing the measurement of each RSB detector's response, dynamic range, nonlinearity, and signal-to-noise ratio (SNR). A linear fit of dn vs. radiance was used for the RSB pre-launch radiometric calibration. The SIS-100 measurements were performed at the three TV instrument temperature plateaus using both the primary and redundant on-board signal control and data acquisition electronic sub-systems. This data was used to characterize system response to changes of the instrument temperature. Because the VIS and NIR FPAs are not actively controlled, their temperatures are closely coupled with (or correlated to) the instrument temperature. Other pre-launch activities included RVS characterization and polarization sensitivity measurements.

Figure 12: MODIS reflective solar bands pre-launch calibration source: SIS-100

The on-board SD panel, shown in Figure 5, is made from space-grade Spectralon™ with a near Lambertian reflectance profile in the VIS/NIR/SWIR regions. The SD bi-directional reflectance factor (BRF) was carefully characterized pre-launch by the instrument vendor using a scattering goniometer in a comparison mode with reference samples traceable to reflectance standards at the National Institute of Standards and Technology (NIST). The SD BRF measurements were made at 400nm, 500nm, 600nm, 700nm, 900nm, and 1700nm over a two-dimensional grid of nine directions of incidence, a combination of 3 elevation and 3 azimuth angles. The incident directions to the SD were chosen to cover the anticipated range that would be observed during on-orbit calibration. The viewing direction of the scan mirror to the SD was fixed during these tests. Additionally, the BRF at 2100nm was indirectly derived from the SD BRF at other wavelengths and total integrated scattering measurements of reference samples. A set of second order polynomials with a functional dependence on the incident direction to the SD described by solar zenith angle θ and solar azimuth angle φ was determined from this pre-launch measured BRF values. For each RSB, a second order polynomial was interpolated from the surface fits at surrounding wavelengths.

4.2 On-orbit Calibration Algorithm (RSB)

Based on the desire of the MODIS science community, the top of the atmosphere (TOA) scene reflectance factor was chosen as the primary L1B data product for the MODIS reflective solar bands (RSB). The on-orbit calibration of the reflectance factor [Xiong et al., 2002b] is based on solar observations via the instrument's on-board solar diffuser (SD).

Using a simple linear algorithm, the Earth view (EV) reflectance factor, $\rho_{EV}\cos(\theta_{EV})$, is related to the detector's response by

$$\rho_{EV} cos(\theta_{EV}) = m_1 \cdot dn_{EV}^* \cdot d_{ES-EV}^2 \tag{4.1}$$

where

ρ_{EV} is the EV scene reflectance.
θ_{EV} is the solar zenith angle of the EV pixel.
m_1 is a calibration coefficient determined from on-orbit SD observations.
d_{ES-EV}^2 is the Earth-Sun distance (in AU) at the time of the EV scene observation.
dn_{EV}^* is the sensor's digital response to the EV scene with background subtracted and instrument effects corrected.

Instrument effect corrections include normalizing the sensor's viewing angle and correcting for the instrumental temperature dependence via

$$dn_{EV}^* = dn_{EV} \cdot (1 + k_{inst} \cdot \Delta T_{inst\_EV})/RVS_{EV} \tag{4.2}$$

where

k_{inst} is the instrument temperature correction coefficient determined pre-launch.
ΔT_{inst_EV} is the difference between the instrument temperature at the time of EV observation and its reference value, $\Delta T_{inst\_EV} = T_{inst\_EV} - T_{inst\_ref}$

T_{inst_EV} is the instrument temperature at the time of EV observation.
T_{inst_ref} is the instrument temperature reference value, chosen pre-launch and used for deriving k_{inst}.
RVS_{EV} is the system level response at the scan angle of an EV pixel.

The dark background subtracted response, dn_{EV}, is computed by

$$dn_{EV} = DN_{EV} - \langle DN_{SV} \rangle \tag{4.3}$$

where DN_{EV} is the EV digital response (raw data) and $\langle DN_{SV} \rangle$ is the average SV digital response. The SD calibration coefficient m_1 is determined by

$$m_1 = \frac{\rho_{SD} cos(\theta_{SD})}{dn_{SD}^{*} \cdot d_{ES\_SD}^{2}} \cdot \Gamma_{SDS} \cdot \Delta_{SD} \tag{4.4}$$

where

ρ_{SD} is the SD pre-launch BRF.
dn_{SD}^{*} is the corrected detector response to the SD.
d_{ES_SD} is the Earth-Sun distance in AU at the time of the SD measurements.
Γ_{SDS} is the SD screen (SDS) vignetting (transmission) function.
Δ_{SD} is the SD degradation factor.

Except for the SD degradation factor, Δ_{SD} and the SD screen (SDS) vignetting function, Γ_{SDS}, equation 4.4 is the same as equation 4.1 when it is applied to the SD observations.

The SD reflectance and MODIS optics transmission deteriorate on-orbit due to their exposure to sunlight [Xiong, et al., 2001 and Xiong et al., 2002c]. The SD degradation rate is tracked by the solar diffuser stability monitor (SDSM) during each SD calibration. The SDSM alternately measures the response of the SD view and a direct Sun view through an attenuation screen of 1.44% nominal transmittance so that the responses from both views are closely matched. Nine individually filtered detectors in the SDSM monitor the SD degradation. The SDSM has 9 Si detectors with wavelengths spanning the visible and NIR, 412 nm to 936 nm. The degradation is calculated at these 9 wavelengths and the results are interpolated to determine the SD degradation at the wavelengths of the VIS and NIR MODIS bands.

The SDSM is not designed to monitor the SD degradation at the SWIR band wavelengths. Early in the MODIS missions, it was reasonable to assume that the SD was not degrading at the SWIR band wavelengths, since the degradation is generally less at longer wavelengths. However, after many years on orbit, the SD degradation at the NIR wavelengths became significant, particularly for Terra (as of June 2017, the SD reflectance at 936 nm has degraded by 2.3%), and degradation at SWIR wavelengths had to be considered. An improved SD degradation at SWIR wavelengths is obtained by fitting a wavelength-dependent model to the SDSM results from the visible and NIR wavelength detectors. [Twedt et al., 2017]

For high gain bands (bands 8-16), a retractable solar diffuser screen (SDS) is placed in front of the SD to attenuate the direct sunlight and to avoid saturation. The SDS attenuation is represented by the vignetting (transmission) function Γ_{SDS}. The vignetting function is set to unity for bands 1-7, 17-19, and 26 when these bands are calibrated without the SDS. Note that beginning July 2, 2003 the Terra RSB calibration includes the SDS, so the vignetting function is no longer set to unity.

The RSB calibration coefficients, m_1, are provided to the L1B software through LUTs. These coefficients are band, detector, sub-sample, and mirror side dependent. They are updated based on regularly scheduled SD/SDSM observations. The MODIS L1B RSB software also produces a radiance product. From the reflectance factor, the Earth view radiance can be calculated by

$$L_{EV} = \frac{\rho_{EV} cos(\theta_{EV}) \cdot E_{Sun}}{\pi d_{ES\_EV}^2} \tag{4.5}$$

where E_{Sun} is the solar irradiance at d = 1 AU, computed at mid-granule. E_{Sun}/π is written as a global attribute in the L1B product so that the users can readily convert the RSB reflectance product to the radiance product.

4.3 Response Versus Scan Angle (RVS)

The MODIS scan mirror scans the Earth view (EV), SD, SRCA, BB, and SV sectors sequentially. As shown in Figure 4b, the EV AOI varies from 10.5^o to 65.5^o with the nadir at the center, AOI 38^o. For the SD, SV, and SRCA, the AOI is 50.25^o, 11.2^o, and 38^o, respectively. The RVS of the MODIS scan mirror for both Terra and Aqua MODIS RSB was measured before launch. The measurements showed that the prelaunch RVS could be approximated as detector independent but was wavelength (band) dependent. It showed a strong mirror side (MS) dependence, especially for Terra MODIS shorter wavelength bands. The on-orbit RVS variation for most MODIS RSB can be tracked accurately by the onboard calibrators, the lunar observations, and EV MS ratios. For a few RSB, mostly at short wavelengths, additional EV observations of pseudo-invariant targets are needed to accurately track RVS changes. On orbit, the RVS cannot be measured in an absolute sense; only relative changes can be measured. The RVS is defined as the pre-launch RVS, RVS_{PL}, multiplied by the on-orbit changes relative to the initial on-orbit measurements, RVS_{oo}:

$$RVS(B, D, MS, \theta, t) = RVS_{PL}(B, MS, \theta) \times RVS_{oo}(B, D, MS, \theta, t), \tag{4.6}$$

where B, D, MS, θ, and t represent the dependence on band, detector, mirror side, AOI, and time. In addition to band and mirror-side dependence measured pre-launch, the on-orbit RVS changes may also depend on detector and change in time. The MODIS RSB RVS is always normalized at the AOI of the SD. Thus, the RVS represents the ratio of the gain at a particular AOI to that at the AOI of the SD.

The gains of the MODIS electronic and optical system at the AOI of the SD and the SV are inversely proportional to the SD calibration coefficients and lunar coefficients, respectively. Thus, RVS on-orbit variation at the AOI of the SV can be derived from the ratio of these two coefficients for both MS1 and MS2. The gain at any other AOI cannot be determined from onboard calibrator data alone. The RVS across all AOI is approximated using a simple linear function to extrapolate the measured gains at the SD and SV to all other AOI. This RVS characterization strategy based on on-board calibrators is termed the OBC-based RVS, has been used in previous MODIS L1B Collections, and continues to be used for many RSB in Collection 7 (Aqua MODIS bands 10-19 and Terra MODIS bands 13-19).

The linear RVS characterization is improved for a few ocean bands (Aqua bands 10-16 and Terra bands 13-16) using MS ratio data from equatorial ocean EV scenes. The MS ratio of the gain for any band, detector, or AOI can be derived from the MS ratio of the instrument's response. From EV observations, the MODIS MS response ratio at any selected AOI can be derived. Although the Earth's surface is not smooth, the EV radiance can be approximated as coming from the same light source for the two mirror sides of the scan mirror when averaged over many scans. The MODIS MS response ratio at the AOIs of the SV, nadir, and SD can also be derived from the lunar, the SRCA, and the SD observations, respectively. For each MS, we only know the RVS on-orbit variation at the AOI of the SD and that of the SV, although we know the MS ratio of the RVS on-orbit variation for all AOI. Knowing the RVS variation at the AOI of the SD and the SV, a linear approximation can be applied for the RVS on-orbit variation as a function of the AOI. In principle, the approximation can be applied to the RVS on-orbit variation for either of the two mirror sides. But for Terra MODIS, the MS differences were already observed in prelaunch measurements and differences exist when the linear approximation is applied to the other mirror side. It is believed that it would be better to apply the linear approximation to the Terra RSB MS1 RVS on-orbit variation. Thus, for Terra MODIS RSB MS1, the RVS on-orbit variation at any AOI is calculated from the RVS at the AOI of the SD and that of SV with a linear approximation for the AOI dependence. Then the MS1 RVS can be obtained by multiplying the prelaunch MS1 RVS and the RVS on-orbit variation. Since the MS ratio of the instrument's response represents the MS ratio of the RVS, Terra MODIS RSB MS2 RVS can be calculated using the MS1 RVS and the MS ratio of the instrument's response obtained from SD, lunar, and EV observations. SRCA MS ratios are no longer used in this calculation because of reduced reliability of the SRCA data in recent years due to continued degradation and failures of the SRCA lamps. The same mirror side convention used for Terra is also applied to Aqua.

For several RSB, data from pseudo-invariant EV targets are used to add adjustments to the calibration on top of the SD and lunar data. The EV-based RVS algorithm was used for some bands in Collection 6 [Sun et al (2014) and Toller et al (2013)] and has been extended in Collection 7 [Twedt et al (2021)]. In the EV-based calibration, the at-launch SD m_1 and pre-launch RVS are still used as the absolute calibration reference at the start of mission, but the on-orbit gain trend is derived from analyzing EV signal trends at multiple view angles to derive an on-orbit gain change $G_{EV}^{oo}(t,\theta)$ covering all AOI. The EV-based calibrated m_1 and RVS are calculated separately for each band and mirror side (using data averaged over all detectors and sub-samples) as

$$\frac{m_1(t)}{RVS(t,\theta)} = \left(\frac{m_1(t_0)}{RVS_{PL}(\theta)}\right)\frac{1}{G_{EV}^{oo}(t,\theta)}, \tag{4.7}$$

where the RVS is still normalized to 1 at the SD AOI.

Regular observations from pseudo-invariant calibration sites in the North African desert, specifically Libya 1, Libya 2, and Libya 4, are utilized for Aqua bands 1-4, 8, and 9, and Terra bands 1-4, and 8-10. The signals from the desert observations are corrected for the site BRF variation using a semi-empirical correction. Additionally, for Terra MODIS only, a correction to the desert data is applied to remove the impact of polarization sensitivity. Terra MODIS had some modest polarization sensitivity in pre-launch testing and has experienced significant on-orbit changes in the polarization sensitivity, the impact of which is mostly evident at the shortest wavelengths. Previously, the NASA Ocean Biology Processing Group (OBPG) developed a correction to account for the polarization effects on the Terra MODIS L1B [Angal 2020]. Starting in Collection 7, the OBPG coefficients are used to correct the desert data before its use in the on-orbit RVS characterization for Terra bands 3-4 and 8-10. While this algorithm ensures that the polarization sensitivity does not adversely impact the Terra L1B calibration, it is important to note that the L1B images will still be impacted by the polarization sensitivity, with the magnitude of the impact varying from scene to scene. In comparison, the short wavelength bands of Aqua MODIS have not shown any changes in the polarization sensitivity on-orbit.

Starting in Collection 7, EV scene data from open ocean scenes and from deep convective clouds are also used in the EV-based RVS calibration for Terra MODIS RSB. The mean reflectance over DCC pixels is calculated at various AOI and is used to derive on-orbit RVS changes for Terra SWIR bands 5 and 26. For the longer wavelength SWIR bands 6 and 7, there is no evidence of RVS changes on-orbit, so the RVS continues to use the static pre-launch values, but the DCC data is still used to apply a correction to the m_1 calibration. The algorithm using the DCC data is nearly the same as the algorithm used for the desert data. In addition, bands 11 and 12 of Terra MODIS use data over open ocean scenes and an intercalibration approach with spectrally matching band 4 as a reference to adjust their RVS calibration.

In practice, for all the bands that use EV-based calibration, the OBC-based calibration using SD and moon is calculated first and then the reflectance of the EV sites is generated using the OBC-based calibration. These reflectance trends show drifts of several percent over the mission depending on band and view angle, indicating the inadequacy of the OBC-based calibration. The reflectance trends are fit over time and AOI, using the assumption of long-term reflectance stability to derive $G_{EV}^{oo}(t,\theta)$ and the final m_1 and RVS LUTs through Eq. 4.7.

For most RSB, the on-orbit RVS changes are detector independent, i.e., the RVS depends only on band, MS, AOI, and time. Data from the SD, Moon, and EV targets are averaged over detectors before they are applied to calculate the RVS. During the early mission, the RVS detector difference was negligible compared to the 2% specified uncertainty in reflectance for MODIS RSB calibration. However, the AOI dependence of the detector difference increased as the missions continued. Starting with Terra MODIS L1B collection 6, the RVS is derived at the individual detector level for a few RSB. In Collection 7, Terra bands 3-4 and 8-12 and Aqua bands 8-12 use detector dependent RVS. The detector-dependence is derived using only SD and lunar data and a linear interpolation across AOI.

In Collection 7, the time-dependent on-orbit RVS has been applied to nearly all RSB. Only the SWIR bands 6-7 for Terra and 5-7 and 26 for Aqua continue to use only the pre-launch RVS. The calculated RVS are fit to a quadratic form for most RSB, whereas a quartic fit is used for some of the bands that use EV data and have more significant RVS changes: Terra bands 3-4 and

8-12 and Aqua bands 1-4 and 8-9. The fitted time-dependent coefficients are applied to calculate the RVS in MODIS L1B products.

4.4 Special Considerations in the RSB Calibration Algorithm

The general RSB algorithm described above applies to the Terra MODIS L1B as well as to the Aqua MODIS L1B. Each L1B code has its own set of LUTs which are instrument specific. There are only minor differences between the two sets of software.

4.4.1 SWIR Crosstalk Correction

Pre-launch and on-orbit characterization of both Terra and Aqua MODIS have shown small but non-negligible out-of-band (OOB) response in the sensors' short-wave infrared bands (SWIR). In general, the Aqua SWIR bands' OOB responses (including the thermal leaks) were much smaller than those for the Terra MODIS. To minimize the impact due to OOB response, a simple linear correction algorithm has been developed, tested, and implemented in the L1B codes for both Terra and Aqua MODIS.

For Terra MODIS, the SWIR band EV data and SD calibration dataset are corrected by the following expression using MODIS band 25:

$$dn'_{EV}(BDSM)_{SWIR} = dn_{EV}(BDSM)_{SWIR} - x\_oob\_1(BDSM)_{SWIR} \cdot dn_{EV}(BDM)_{B25} \tag{4.8}$$

where

BDSM is a band, detector, sub-sample, and mirror side index (respectively) used in the RSB calibration.

$dn'_{EV}(BDSM)_{SWIR}$ is the response of the receiver SWIR band after correction for OOB crosstalk.

$dn_{EV}(BDSM)_{SWIR}$ is the response of the receiver SWIR band before correction for OOB crosstalk.

$x\_oob\_1(BDSM)_{SWIR}$ is the thermal leak correction coefficient.

$dn_{EV}(BDM)_{B25}$ is the response of the sender band, band 25 in this case.

Because there is no sub-sample in B25 (1km spatial resolution band with 10 detectors), B25 detector 1 is matched with B5, B6 and B7 detectors 1 and 2 (both sub-samples), B25 detector 2 is matched with B5, B6 and B7 detectors 3 and 4, etc. The same algorithm is also used in Aqua MODIS L1B. The choice of the sending band is based on OOB characterization, on-orbit observations, and science test results. The correction coefficients are derived from on-orbit observations. For Terra MODIS, all previous collections before C6.1 utilized 28 as the sending band for this correction. However, due to increased crosstalk behavior within the MWIR bands after the 2016 safe mode event, the sending band was switched to B25 in July 2019 (same band as Aqua MODIS). A time-dependence was also implemented to the x_oob_1 coefficient at this time, impacting the m1 and RVS LUTs. No changes were made to the L1B algorithm.

In addition to the thermal leak, the SWIR bands also have electronic crosstalk that has made this problem difficult to characterize and correct. To distinguish the electronic crosstalk among the SWIR detectors from that coming from the MWIR detectors, a special instrument activity to collect the Earth scene RSB (including SWIR bands) data during spacecraft nighttime is used. This is designated the nighttime day mode (NTDM). The thermal leak correction coefficients are derived by fitting the SWIR responses to the corresponding sending band.

4.4.2 B26 De-striping Algorithm

A de-striping algorithm was furnished by the atmospheric group at the University of Wisconsin. It only applies to MODIS band 26. It is a simple linear approach developed to remove the difference (striping) among the 10 detectors in band 26. The coefficients are derived from the L1B EV scaled integers of band 26 and band 5 after the SWIR crosstalk correction algorithm [Moeller, C., 2001].

4.4.3 Aqua Band 6 Consideration

Prior to launch, most of the Aqua Band 6 detectors were known to be non-functional. This information is communicated to L1B from the LUTs. As with all non-functional detectors, the bad channels are not used in the data products.

4.4.4 Moon in the SV Port

Typically, the SV signal is subtracted as in equation 4.3. However, the SV digital counts are unreliable if the Moon is in the SV port. When this occurs, the SV digital counts are sorted and a few (defined in the LUT) of the lowest readings are used. If no valid SV digital count is obtained, the RSB use the on-board BB as the background, replacing the SV readings, except for the SWIR bands.

4.4.5 DN saturation

Both Aqua and Terra MODIS have RSBs impacted by pre-saturation, i.e. they reach saturation before the maximum 4095 DN. This has been known prior to launch, with Terra MODIS bands 1, 2, and 17 and Aqua MODIS bands 2, 15, 17 and 19 being impacted. The saturation LUT utilizes 1 full orbit of the L1A Earth view product to generate a histogram and determine the DN at which saturation occurs for the listed bands. This is accomplished by applying a moving-window average fit to the measured DN saturation values and generating one LUT each calendar year (timestamps of YYYY001). These LUTs are applied to the L1B product using a step function.

4.5 Uncertainty (RSB)

MODIS L1B data products also include uncertainty indices that are computed for all pixels. The RSB uncertainty algorithm is based on characterization of the EV scene reflectance.

The RSB reflectance total uncertainty can be expressed as

$$\left[\frac{\delta(\rho_{EV}\cos(\theta_{EV}))}{\rho_{EV}\cos(\theta_{EV})}\right]_{EV}^2 = \left[\frac{\delta(m_1/RVS)}{m_1/RVS}\right]^2 + [\delta(k_{Inst}\Delta T_{Inst})]^2 + \left[\frac{\delta dn_{EV}}{dn_{EV}}\right]^2. \tag{4.9}$$

The first term on the right side is the calibration uncertainty, calculated from the uncertainty of the SD/SDSM calibration, the lunar calibration, and EV response trending. The second term is the uncertainty of the temperature correction, and the last term addresses the scene dependent uncertainty due to instrument noise. In Collection 7, the calibration coefficients are derived from the SD/SDSM calibration and the RVS are derived from the SD/SDSM and lunar observation with support from EV mirror side ratio for most MODIS RSB. But for several Terra and Aqua bands, the EV response trending over selected EV targets is also used to derive the calibration coefficients and RVS LUT as discussed in Section 4.3. Then the uncertainty of the calibration can be calculated from the uncertainty of the SD/SDSM calibration, lunar calibration, and EV response trending. The determination of the individual RSB uncertainties at L_{typ} is described by Xiong et.al (2018)

The various components contributing to the MODIS RSB uncertainty algorithm are organized in five different terms, each with its own LUT (U1, U2, U3, U4, and U5), when computing the uncertainty of the RSB L1B product. The organization is based on each term's dependence of band, detector, mirror side, sub-frame, time, AOI, and scene:

$$\left[\frac{\delta(\rho_{EV}\cos(\theta_{EV}))}{\rho_{EV}\cos(\theta_{EV})}\right]_{EV}^2 = U_1(B,D)^2 + U_2(B,D,MS,\theta,t)^2 + U_3(B,D,M)^2 + U_4(B,D,MS,SF,t,scene)^2 + U_5(B,D,MS,SF,t,scene)^2. \tag{4.10}$$

The first term, U1, contains the terms of the SD calibration uncertainty that are constant in time. The second term, U2, represents the RVS uncertainty as well as uncertainty in the m_1 not accounted for in U1. The U2 term is both time- and AOI-dependent and varies depending on the band and whether the on-board RVS algorithm or the EV-based RVS algorithm is used. The third term, U3, represents the uncertainty in the instrument temperature correction. The fourth term, U4, contains the scene-dependent uncertainty in dn_{EV} and is derived from the SD calibration measurements. The final term, U5, is an additional term, not derived from the above equations, that accounts for uncertainty due to optical leak and electronic crosstalk in the SWIR bands. It is assigned to be equal to ¼ of the SWIR dn_{EV} correction ($\Delta dn_{EV}/dn_{EV}$). At typical radiance levels for both sending and receiving bands, this term (averaged over operable detectors and sub-frames) could be from 0.2% to 2.0% for Terra MODIS SWIR bands with the largest uncertainty for band 5. With less optical leak and electronic crosstalk, the Aqua SWIR band uncertainty is smaller than for Terra MODIS.

5. LEVEL 1B DATA PRODUCTS AND ALGORITHM IMPLEMENTATION

5.1 L1B Data Products

The sensors' raw data are transmitted to ground stations, such as the one at White Sands in New Mexico, through the Tracking Data Relay Satellite System (TDRSS) and then sent to the EOS Data and Operations System (EDOS). At the Goddard Space Flight Center Distributed Active Archive Center (GDAAC), the sensor's original binary data files (Level 0) from the EDOS are reformatted, attitude and ephemeris data are incorporated, and the data is separated into 2-hour Level 0 files. Starting in 2006, the GDAAC passed these Terra and Aqua 2-hour Level 0 files to the MODIS Adaptive Processing System (MODAPS) which produces Level 1A (L1A) granules using EOS specific Hierarchical Data Format (HDF). Each L1A granule contains 5 minutes of data, consisting of the sensor's response in digital numbers (DNs) as well as other engineering and telemetry information. These are the principal inputs to the Level 1B (L1B) process. Other inputs include a geolocation file and a set of L1B Look-Up Tables (LUTs) that provide parameters determined during pre-launch and on-orbit calibration and characterization. The MODIS L1B products are distributed through the Level 1 and Atmosphere and Archive Distribution System available at http://ladsweb.nascom.nasa.gov.

L1B output consists of calibrated Earth View (EV) data for all 36 spectral bands, organized in three product files corresponding to MODIS' three spatial resolutions, and associated metadata files. These files serve as the common input for all higher-level science algorithms. The L1B process also produces a separate file containing on-board calibration data sets and key instrument telemetry. The latter does not contain the EV sector data and is primarily used by MCST analysts to perform instrument on-orbit calibration and to monitor the instrument's status. The format of these files is the widely used Hierarchical Data Format (HDF). HDF4 and HDF-EOS2 were used prior to Collection 7. To produce continuous data records in a consistent data format with the MODIS follow-on instrument, Visible infrared Imaging Radiometer Suite (VIIRS), NetCDF-4/HDF5 and HDF-EOS5 are chosen to be used in all MODIS products from Collection 7.

The Level 1B calibrated EV data products include top of the atmosphere (TOA) reflectance factors for the RSBs, TOA radiances for both the RSBs and TEBs, associated uncertainty indices and data quality flags. To reduce file size, the calibrated Earth view data are stored as 16-bit unsigned integers coupled with associated scale and offset terms in three separate product files (see Appendices B and C). This approach allows the user to reconstruct calibrated radiance values for all MODIS bands as well as calibrated reflectance values for the Reflective Solar Bands (RSBs). Associated uncertainty values are included as unsigned 8-bit integers with coefficients provided to reconstruct the percent uncertainty. A scan-by-scan 32-bit data quality flag and a granule level 8-bit detector quality flag for each of the 490 detectors are included as part of each file's metadata.

5.2 L1B Algorithm Implementation

MODIS L1B software provides calibration for all TEB and RSB detectors. Calibration is performed for each band, detector, sub-sample (for the sub-kilometer resolution bands 1-7), and mirror side (BDSM), and thus is on a pixel-by-pixel basis for all MODIS detectors. The radiometric calibration algorithm is divided into two major modules in the L1B software: one for the thermal emissive bands and the other for the reflective solar bands. The RSB calibration uses some processed data from TEB calibration and is therefore performed after the TEB calibration. Both TEB and RSB calibration modules in the L1B process are executed after L1B pre-processing in which the calibration coefficients are either calculated from on-orbit data sets or determined from the associated LUT inputs.

Figure 14 [Xiong et al., 2005b] is a simplified flow diagram that illustrates the core of the TEB calibration algorithm: computing the EV radiance, converting radiance to a scaled integer (SI), and computing the uncertainty index (UI). For each scan of EV data, this process loops through bands, detectors, and frames. The data quality flags are assigned for each scan of the data. In the TEB calibration, an electronic crosstalk correction (PVX) is applied to bands 20-25 (MWIR) and 27-30 (LWIR), and an optical crosstalk (PCX) correction algorithm is applied to bands 32-36. Based on the sensors' calibration and characterization results, the PVX switch is set to "ON" for both Terra and Aqua MODIS L1B, the PCX switch is set to "ON" for Terra MODIS L1B and "OFF" for Aqua MODIS L1B. The PVX and PCX coefficients are provided by the LUTs. MODIS Band 21, which is primarily used for fire detection and has extremely low gain, also uses calibration coefficients from the LUTs. For Aqua MODIS, LUTs also provide calibration coefficients for bands 33, 35, and 36 when the on-board calibrator blackbody radiance (temperature) is above these bands' saturation limits.

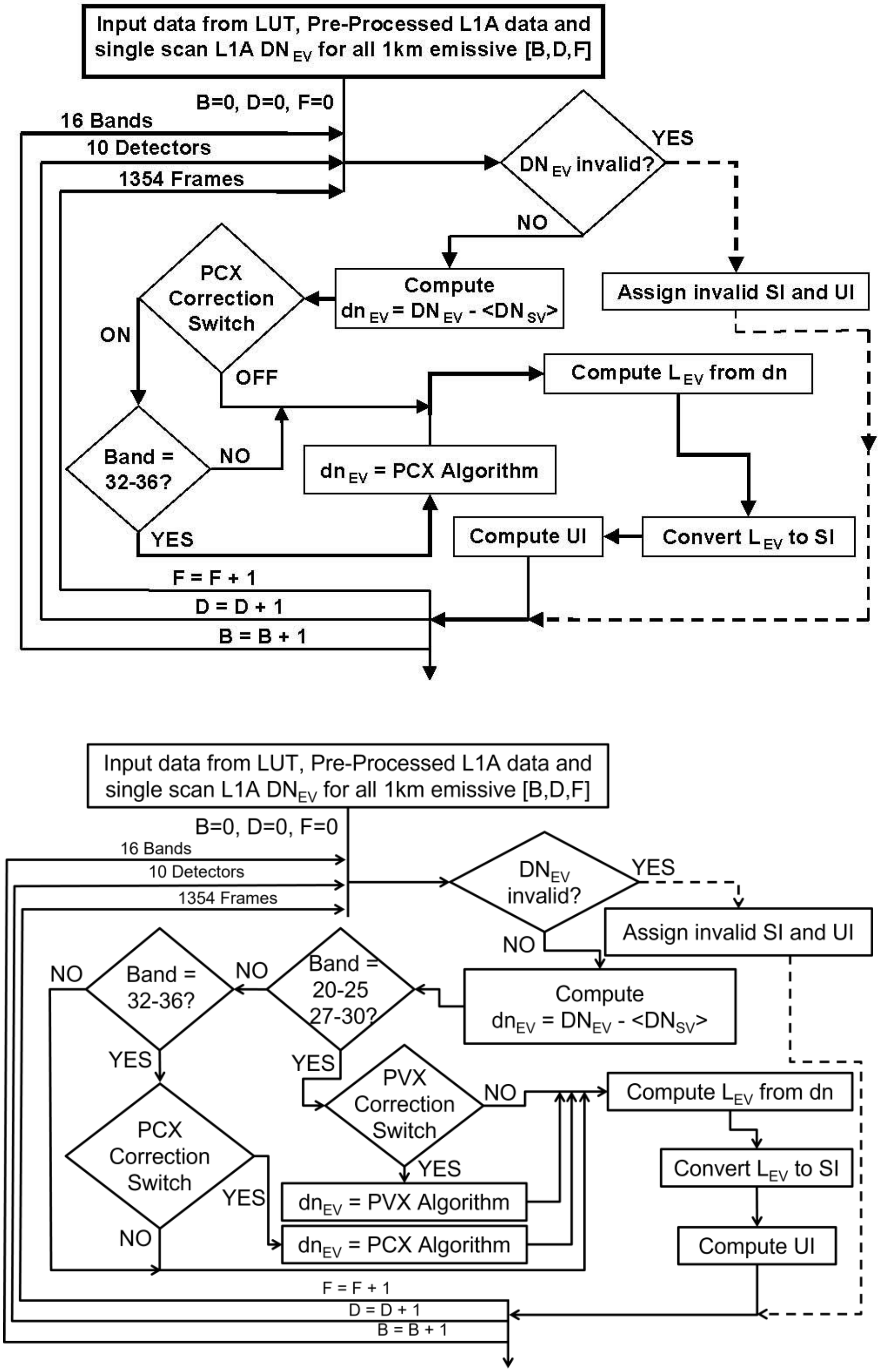

Figure 14: Thermal Emissive Band L1B Flow Diagram

Figure 15 [Xiong et al., 2005b] shows the flow diagram of the RSB calibration module which is executed after the TEB calibration module. Compared to the TEB calibration, an extra loop is added for the bands/detectors with sub-frames (Bands 1-7). For the Short-Wave Infrared (SWIR) bands (5-7 and 26), the algorithm includes a thermal leak correction that is applied to both the Terra and Aqua MODIS data. Some of the data used in the SWIR thermal leak correction comes from the already processed TEB data.

Following the radiometric calibration of each granule, a set of band dependent scale and offset terms are calculated and written into L1B output as scientific data set (SDS) attributes that are used to reconstruct the radiance and reflectance values from the scaled integers. In each data set, the RSB radiance values can also be derived from the reflectance factors using the global attributes "Earth-Sun Distance" and "Solar Irradiance on RSB Detectors over pi". The solar irradiance is weighted by the relative spectral response (RSR) of each RSB detector. The MODIS Level 1B Product User's Guide provides the detailed description of this process [MCST, 2003c].

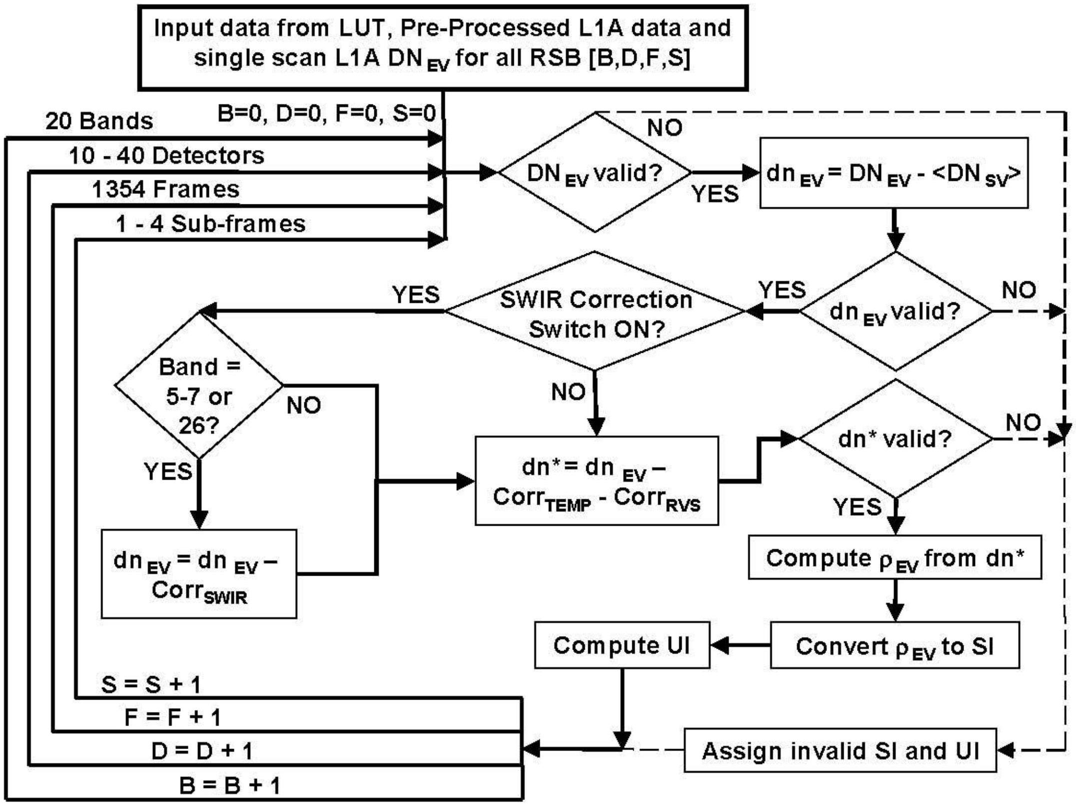

Figure 15: Reflective Solar Band L1B flow diagram

5.3 L1B Data Product Retrieval

The calibrated MODIS Earth view data are stored as scaled integer (SI) scientific data sets (SDS) within the Level 1B output files. The output files also contain scale and offset terms stored as attributes which enable the user to convert the calibrated data to TOA radiances and, in the case of the Reflective Solar Bands, to TOA reflectance factors. The following expressions are used to convert the SI to the scene TOA radiances or reflectance factors.

For the TEB radiance:

$$Radiance = radiance\_scales * (SI - radiance\_offsets)\,. \tag{5.1}$$

For the RSB reflectance factor:

$$Reflectance = reflectance\_scales * (SI - reflectance\_offsets)\,. \tag{5.2}$$

For the RSB radiance:

$$Radiance = Reflectance \cdot \frac{Solar\_Irradiance\_over\_pi}{(Earth - Sun\_Distance)^2}\,. \tag{5.3}$$

For the thermal emissive bands, the radiance scale and offset terms are used to reconstruct the radiance values calculated within the Level 1B TEB calibration algorithm. For the reflective solar bands, the reflectance scales and offsets may be used to reconstruct the reflectance factors calculated within the RSB calibration algorithm, but use of the radiance scales and offsets for the reflective solar bands will result in only approximate radiance retrievals. This is because the reflective radiance scales are derived using a band-averaged value of the solar irradiance, which actually varies from detector to detector due to the individual detector's relative spectral response (RSR) function. An alternative method to derive RSB radiances, which yields more precise results, is to use the global attributes "Earth-Sun Distance" and "Solar Irradiance on RSB Detectors over pi" to reconstruct the radiances directly from reflectance values. This method is given by equation 5.3.

To cover a broad range of uncertainty in percentage for the retrieved EV products, an exponential approach is used. Two SDS attributes, "specified_uncertainty" and "scaling_factor" in equation 5.4, are used to convert the Uncertainty Index (UI) back to the percentage uncertainty. Additional information is provided in the MODIS Level 1B Product User's Guide [MCST, 2003c].

$$Uncertainty\ (\%) = Specified\_uncertainty \cdot exp\left(\frac{UI}{Scaling\_factor}\right). \tag{5.4}$$

6. SUMMARY

MODIS, a key instrument for the NASA's EOS and MTPE missions, is currently operating on both the Terra and Aqua spacecraft, providing continuous global data sets from complementing morning and afternoon observations of the Earth's land, oceans, and atmosphere. MODIS has 36 spectral bands covering spectral regions from the VIS to LWIR (0.41 to 14.5μm), taking observations at 250m, 500m, and 1km nadir spatial resolutions. Ongoing monitoring of instrument operation and performance of comprehensive calibration and characterization has shown both Terra and Aqua MODIS are performing well. The mature, validated MODIS L1B algorithms are used to generate calibrated L1B products. Updates that account for changes in sensor performance are implemented via numerous L1B LUTs. The two MODIS instruments are identical in many aspects, allowing a common calibration approach for generation of the L1B data products with special treatments added in the code to account for differences in the two sensors. For additional information on the MODIS instrument calibration and characterization, current instrument status, L1B code changes, and LUT updates, please use the MODIS Characterization Support Team (MCST) web page (http://mcst.gsfc.nasa.gov/).

7. REFERENCES

Angal, A., X. Geng, X. Xiong, K. Twedt, A. Wu, D. Link, and E. Aldoretta, "On-Orbit Calibration of Terra MODIS VIS Bands Using Polarization-Corrected Desert Observations", IEEE Transactions on Geoscience and Remote Sensing, vol. 58, issue 8, pp. 5428-5439, 2020.

Barker, J., J. Harnden, H. Montgomery, P. Anuta, G. Kavaran, E. Knight, T. Bryant, A. McKay, J. Smid, and D. Knowles, MODIS Level 1 Geolocation, Characterization and Calibration Algorithm Theoretical Basis Document, Version 1, Goddard Space Flight Center, Greenbelt, MD., 1994.

Barnes, W. L., T. S. Pagano, and V. V. Salomonson, Pre-launch characteristics of the Moderate Resolution Imaging Spectroradiometer (MODIS) on EOS-AM1, IEEE Trans. Geosci. Remote Sensing, 36, pp. 1088-1100, 1998.

Barnes, W., X. Xiong, B. Guenther, and V. Salomonson, Development, Characterization and Performance of the EOS MODIS Sensors, Proceedings of SPIE – Earth Observing Systems VIII, W. L. Barnes, ed., 5151, pp.337-345, 2003.

Chang, T., A. Shrestha, P. C. Diaz, N. Chen, A. Wu, T. Wilson, Y. Li, and X. Xiong, "MODIS thermal emissive bands calibration improvements for Collection 7", Proc. SPIE 11858, Sensors, Systems, and Next-Generation Satellites XXV, pp. 118580R, 2021.

Chang, T., X. Xiong, A. Shrestha, and P. C. Diaz, "Normalization method and application for MODIS TEB assessments using Earth scene measurements", Earth and Space Science, vol. 8, issue 5, pp. e2020EA001539, 2021.

EOS, Functional and Performance Requirements Specification For the Earth Observing System Data and Information System (EOSDIS) Core System, NASA, 1994.

Goldberg, I. L., Two-point calibration of non-linear PC HgCdTe channels, Infrared Phys.

Technol., 36, 1995.

GSFC, Specification for the Moderate-Resolution Imaging Spectroradiometer (MODIS), GSFC 422-20-02, Rev. A, March 24, 1993.

Guenther, B., H. Montgomery, P. Abel, J. Barker, W. Barnes, P. Anuta, J. Baden, L. Carpenter, E. Knight, G. Godden, M. Hopkins, M. Jones, D. Knowles, S. Sinkfield, B. Veiga, N. Che, L. Goldberg, M. Maxwell, T. Zukowski, T. Pagano, N. Therrien, and J. Young, MODIS Level 1B Algorithm Theoretical Basis Document [MOD-02], GSFC, Greenbelt Maryland, 1995.

Guenther, B. W. Barnes, E. Knight, J. Barker, J. Harnden, G. Godden, H. Montgomery, and P. Abel, MODIS Calibration: A Brief Review of the Strategy for the At-Launch Calibration Approach, J. Atmos. Ocean. Tech., 13, 274-285, 1996.

Isaacman, A. G. Toller, B. Guenther, W. Barnes, and X. Xiong, MODIS Level 1B Calibration and Data Products, Proceedings of SPIE – Earth Observing Systems VIII, 5151, 552-562, 2003. http://dx.doi.org/10.1117/12.507957

Madhavan, S., A. Wu, K. Chiang, and Z. Wang, "MODIS TEB Uncertainty Algorithm Collection 6 Update", MCST memo M1153, Feb. 8, 2013.

MCST Home Page, http://mcst.gsfc.nasa.gov, accessed February 21, 2025.

MCST, MODIS Level 1B Algorithm Theoretical Basis Document, Version 2, Goddard Space Flight Center, Greenbelt MD, May 1997.

MCST, MODIS Level 1B Algorithm Theoretical Basis Document, Version 3, Goddard Space Flight Center, Greenbelt MD, December 2005.

MCST, MODIS Level 1B Algorithm Theoretical Basis Document, Version 4, Goddard Space Flight Center, Greenbelt MD, June 2013.

MCST, MODIS Level 1B In-Granule Calibration Code (MOD_PRO2) High-Level Design, applicable to Level 1B code version 6.1.14 (MODIS/Terra) and version 6.1.17 (Terra/Aqua), http://mcst.gsfc.nasa.gov/content/l1b-documents, Goddard Space Flight Center, Greenbelt MD, 2012a.

MCST, MODIS Level 1B Product Data Dictionary, MODIS Characterization Support Team, "MODIS Level 1B Products Data Dictionary- applicable to Level 1B code Version 6.1.14, file specifications Version 6.1.14. (MODIS/Terra) and to Level 1B code Version 6.1.17, file specifications Version 6.1.17 (MODIS/Aqua)", MCM-02-2.3.1-PROC-L1BPDD-U-01-0107-REV D, http://mcst.gsfc.nasa.gov/content/l1b-documents, Goddard Space Flight Center, Greenbelt MD, 2012b.

MCST, MODIS Level 1B Product User's Guide, MCM-PUB-01-U-0202-Rev D, applicable to Level 1B code version 6.1.14 (MODIS/Terra) and version 6.1.17 (Terra/Aqua), http://mcst.gsfc.nasa.gov/content/l1b-documents, Goddard Space Flight Center, Greenbelt MD, 2012c.

MCST, MODIS LUT Information Guide, applicable to Level 1B code version 6.1.14 (MODIS/Terra) and version 6.1.17 (Terra/Aqua), http://mcst.gsfc.nasa.gov/content/l1b-documents, Goddard Space Flight Center, Greenbelt MD, 2012d.

Moeller, C., MODIS B26 Performance Part III, Influence of B5 (1.2 µm) on B26 (1.38 µm), MODIS Science Team Meeting, 12/17/2001.

Nishihama, M., R. Wolfe, D. Solomon, F. Patt, J. Blanchette, A. Fleig, and E. Masuoka, MODIS Level 1A Earth Location: Algorithm Theoretical Basis Document Version 3.0, NASA Goddard Space Flight Center, Greenbelt MD, 1997.

Pérez Díaz, C. L., et al., "An update to the calibration algorithm of the MODIS PV LWIR bands for Collection 7 to improve long-term records," in Proceedings of SPIE 13267, p. 132670Y, 2025.

SBRS, Operational In-Flight Calibrations Procedures, CDRL 404, Hughes Santa Barbara Research Center, Santa Barbara California, 1993.

SBRS, Moderate Resolution Imaging Spectroradiometer (MODIS) Program Calibration Management Plan, SBRC, Goleta, California, 1994.

Sun, J., A. Angal, X. Xiong, H. Chen, X. Geng, A. Wu, T. Choi, and M. Chu, "MODIS Reflective Solar Bands Calibration Improvements in Collection 6", *Proc. SPIE 8528, Earth Observing Missions and Sensors: Development, Implementation and Characterization II, 85280N*, 2012.

Toller, G., X. Xiong, K. Chiang, J. Kuyper, J. Sun, L. Tan, and W. Barnes, Status of Earth Observing System Terra and Aqua MODIS Level 1B Algorithm, *J. Appl. Remote Sens.,* Vol. 2, 023505, http://dx.doi.org/10.1117/1.2839442 , 2008.

Toller, G., X. Xiong, J. Sun, B. N. Wenny, X. Geng, J. Kuyper, A. Angal, H. Chen, S. Madhavan, and A. Wu, Terra and Aqua Moderate-resolution Imaging Spectroradiometer Collection 6 Level 1B Algorithm, *J. Appl. Remote Sens.*, Vol. 7(1), 073557 (May 22, 2013), doi: 10.1117/1.JRS.7.073557, http://dx.doi.org/10.1117/1.JRS.7.073557 , 2013.

Twedt, K., E. Aldoretta, A. Angal, H. Chen, X. Geng, Y. Li, Q. Mu, K. Vermeesch, and X. Xiong, "MODIS reflective solar bands calibration improvements for Collection 7", Proc. SPIE 11858, Sensors, Systems, and Next-Generation Satellites XXV, pp. 118580S, 2021.

Wenny, B.N., A. Wu, S. Madhavan, Z. Wang, Y. Li, N. Chen, K. Chiang, and X. Xiong, MODIS TEB calibration approach in collection 6, Proceedings of SPIE- Sensors, Systems and Next-Generation Satellites XVI, Vol. 8533, doi 10.1117/12.974231, 2012.

Xiong, X., J. Esposito, J. Sun, C. Pan, B. Guenther, and W. Barnes, Degradation of MODIS Optics and Its Reflective Solar Bands Calibration, Proceedings of SPIE – Sensors, Systems, and Next Generation Satellite V, 4540, 62-70, 2001.

Xiong, X., K. Chiang, B. Guenther, and W. L. Barnes, MODIS Thermal Emissive Bands Calibration Algorithm and On-orbit Performance, Proceedings of SPIE – Optical Remote Sensing of the Atmosphere and Clouds III, 4891, 392-401, 2002a.

Xiong, X., J. Sun, J. Esposito, B. Guenther, and W. Barnes, MODIS Reflective Solar Bands Calibration Algorithm and On-orbit Performance, Proceedings of SPIE – Optical Remote Sensing of the Atmosphere and Clouds III, 4891, 392-401, 2002b.

Xiong, X., A. Wu, J. Esposito, J. Sun, N. Che, B. Guenther, W. Barnes, Trending Results of MODIS Optics On-orbit Degradation, Proceedings of SPIE – Earth Observing Systems VII, 4814, 2002c.

Xiong, X., and W. Barnes, MODIS calibration and characterization, Earth Science Satellite Remote Sensing, J. Qu, W. Gao, M. Kafatos, R. Murphy, and V. Salomonson, eds., Vol. I, Chapter 4, Springer-Verlag, New York, 2005a.

Xiong, X., A. Isaacman, and W. Barnes, MODIS level 1B products, Earth Science Satellite Remote Sensing, J. Qu, W. Gao, M. Kafatos, R. Murphy, and V. Salomonson, eds., Vol. II, Chapter 6, Springer-Verlag, New York, 2005b.

Xiong, X., and W. Barnes, MODIS Calibration and Characterization, Earth Science Satellite Remote Sensing, Data, Computational Processing, and Tools, J. J. Qu, W. Gao, M. Kafatos, R. E. Murphy, and V. V. Salomonson, eds., Vol. II, Springer-Verlag, New York, 77-97, 2006.

Xiong, X., B. N. Wenny, and W. L. Barnes, Overview of NASA Earth Observing Systems Terra and Aqua Moderate Resolution Imaging Spectroradiometer Instrument Calibration Algorithms and On-orbit Performance, J. Appl. Remote Sens., Vol. 3, 032501, doi:10.1117/1.3180864, 2009.

Xiong, X., A. Angal, W. L. Barnes, H. Chen, V. Chiang, X. Geng, Y. Li, K. Twedt, Z. Wang, T. Wilson, et al., "Updates of Moderate Resolution Imaging Spectroradiometer on-orbit calibration uncertainty assessments", Journal of Applied Remote Sensing, vol. 12(3),034001, 2018.

Young, J. B., SRCA Spectral Calibration Methodology, PL3095-No4744, March 20, 1995a.

Young, J. B., SRCA along track SBR Modeling/algorithm, PL3095-No4214, August 24, 1995b.

8. APPENDIX A: MODIS SPECIFICATIONS AND DESIGN PARAMETERS

Orbit: 705 km, 10:30 a.m. descending node (Terra) , 1:30 p.m. ascending node (Aqua), sun-synchronous, near-polar, circular orbit
Scan Rate: 20.3 rpm, cross track
Swath Dimensions: 2330 km (across track) by 10 km (along track at nadir)
Telescope: 17.78 cm diam. Off-axis, afocal (collimated), with intermediate field stop
Size, Weight, and Power: 1.0 x 1.6 x 1.0 m, 250 kg, 225 W (orbital average)
Data Rate: 11 Mbps (peak daytime)
Quantization: 12 bits
Spatial Resolution: At Nadir: 250 m (bands 1-2), 500 m (bands 3-7), 1000 m (bands 8-36)
Design Life: 5 years

Primary Use	**Band**	**CW[1]**	**Bandwidth[2]**	**Spectral Radiance[3]**	**Required SNR[4]**
Land/Cloud Boundaries	1	645	620-670	21.8	128
	2	858	841-876	24.7	201
Land/Cloud Properties	3	469	459-479	35.3	243
	4	555	545-565	29.0	228
	5	1240	1230-1250	5.4	74
	6	1640	1628-1652	7.3	275
	7	2130	2105-2155	1.0	110
Ocean Color/Phytoplankton/ Biogeochemistry	8	412	405-420	44.9	880
	9	443	438-448	41.9	838
	10	488	483-493	32.1	802
	11	531	526-536	27.9	754
	12	551	546-556	21.0	750
	13	667	662-672	9.5	910
	14	678	673-683	8.7	1087
	15	748	743-753	10.2	586
	16	869	862-877	6.2	516
Atmospheric Water Vapor	17	905	890-920	10.0	167
	18	936	931-941	3.6	57
	19	940	915-965	15.0	250
Primary Use	**Band**	**CW[1]**	**Bandwidth[2]**	**Spectral Radiance[3]**	**Required NEΔT(K)[5]**
Surface/Cloud Temperature	20	3.75	3.660-3.840	0.45	0.05
	21	3.96	3.929-3.989	2.38	0.20
	22	3.96	3.929-3.989	0.67	0.07
	23	4.05	4.020-4.080	0.79	0.07
Atmospheric Temperature	24	4.47	4.433-4.498	0.17	0.25
	25	4.52	4.482-4.549	0.59	0.25
Cirrus Clouds	26	1375	1.360-1.390	6.00	150[4]
Water Vapor	27	6.72	6.535-6.895	1.16	0.25
	28	7.33	7.175-7.475	2.18	0.25
	29	8.55	8.400-8.700	9.58	0.05
Ozone	30	9.73	9.580-9.880	3.69	0.25
Surface/Cloud Temperature	31	11.03	10.780-11.280	9.55	0.05
	32	12.02	11.770-12.270	8.94	0.05

Cloud Top Altitude	33	13.34	13.185-13.485	4.52	0.25
	34	13.64	13.485-13.785	3.76	0.25
	35	13.94	13.785-14.085	3.11	0.25
	36	14.24	14.085-14.385	2.08	0.35

Appendix A Notes

1. Central Wavelength (nm for bands 1-19, 26; µm for bands 20-25, 27-36)
2. Units: Bands 1 to 19, nm; Bands 20-36 µm
3. (W/m^2 µm sr) Typical Earth scene radiance, L_{typ}
4. SNR = Signal-to-noise ratio {Performance goal is 30% -40% better than required.}
5. NEΔT = Noise-equivalent temperature difference

9. APPENDIX B: L1B TEB SCALED INTEGERS

In the L1B code, the TEB radiance produced for each Earth view (EV) pixel is expressed in a 32-bit floating-point format. It is output as a 16-bit scaled integer (SI) in the Scientific Data Sets (SDS) of the Hierarchical Data Format (HDF) for the L1B data products. The dynamic range of valid data in SI is [0, 32767] and any values greater than 32767 represent invalid data. To convert the SI back to the calibrated radiance for a given pixel, simply use the following expression:

$$L = radiance\_scales(B)[SI - radiance\_offsets(B)]\,. \qquad (9.1)$$

where

$$radiance\_scales(B) = [L_{MAX}(B) - L_{MIN}(B)]\,/\,32767$$

(9.2)

and

$$radiance\_offsets(B) = -32767 L_{MIN}(B)\,/\,[L_{MAX}(B) - L_{MIN}(B)] \qquad (9.3)$$

The values of radiance_scales(B) and radiance_offsets(B) are computed inside L1B based on the L_{MAX}(B) and L_{MIN}(B) values of each band stored in the L1B LUTs. They are written as attributes to the SDS.

10. APPENDIX C: L1B RSB SCALED INTEGERS

In L1B, the RSB product is Earth view reflectance, expressed in a 32-bit floating-point format for each pixel. As with the TEB radiance, the RSB reflectance is output as a 16-bit SI in the SDS of the HDF. The reflectance can be calculated from the SI by

$$\rho_{EV} Cos(\theta_{EV}) = \text{reflectance\_scale(B) [SI - reflectance\_offset(B)]}, \qquad (10.1)$$

where ρ $\cos(\theta_{EV})$ is the EV scene reflectance factor for the EV pixel at solar zenith angle θ_{EV}. reflectance_scale(B) and reflectance_offset(B) are written as attributes to the SDS. With the reflectance, the RSB radiance can be obtained by

$$L_{EV} = \rho_{EV}\cos(\theta_{EV})E_{sun} / \pi d^2_{ES\_EV} \tag{10.2}$$

where E_{sun} is the solar irradiance. The quantity E_{sun}/π for each detector is written as a global attribute to the SDS.

11. APPENDIX D: UNCERTAINTY INDEX IN THE L1B PRODUCTS

After the radiometric uncertainty calculation, a Root-Sum-Square (RSS) approach is completed and the uncertainty is written to the L1B products in terms of the Uncertainty Index (UI) for each pixel, with an integer ranging from 0 to 15. The UI is computed in the L1B using the following expression:

$$UI = scaling\_factor[B] \cdot ln\left(\frac{RSS}{specified\_uncertainty[B]}\right) \tag{11.1}$$

The use of nonlinear log scaling allows a broad range of uncertainty to be covered while an adequate resolution for small uncertainties is still retained. Table 2 lists the band dependent scaling_factor[B] and specified_uncertainty[B] values. They are provided from LUT inputs. The RSS uncertainty is computed dynamically for each pixel in each scan as described above.

12. APPENDIX E: ACRONYMS AND ABBREVIATIONS

a0	Temperature-dependent Offset for TEB Calibration
a2	Temperature-dependent Quadratic Coefficient for TEB Calibration
A/D	Analog-to-Digital Converter
AM-1	Ante Meridian EOS Platform (Terra)
AOI	Angle of Incidence
Aqua	FM1 satellite that houses MODIS
ATBD	Algorithm Theoretical Basis Document
AU	Astronomical Unit
AVHRR	Advanced Very High Resolution Radiometer
b_1	Linear Gain Term for TEB Calibration
BB	OBC Blackbody
BCS	Blackbody Calibration Source
BDSM	Band, Detector, Subframe (sample), Mirror side
BRDF	Bi-Directional Reflectance Distribution Function
BRF	Bi-Directional Reflectance Factor

CFPA	Cold Focal Plane Assembly
CLAM	Cooler Located Amplifier Module
CZCS	Coastal Zone Color Scanner
DAAC	Distributed Active Archive Center
DC	Direct Current
DCR	DC Restore
DN	Digital Number. Raw signal recorded including SV with DCR.
dn	DN Corrected for Electronic Background (i.e., DN-SV)
dn*	DN Corrected for Instrumental Effects and Electronic Background
dn**	For RSB, dn* as Scaled to the SI Within a Defined Dynamic Range so that a Single Set of Calibration Parameters Applies to Every Detector in a Band
ECAL	Electronics Calibration
EM	Engineering Model
Esun	RSR-Weighted Solar Irradiance
EV	Earth view
FAM	Forward Viewing Analog Module
FDDI	Fiber Distributed Data Interface
FIFO	First-In First-Out
FM-1	Flight Model-1 (Aqua)
FPA	Focal Plane Assembly
Frame Number	1-1354. Linearly Related to Scan Angle. An Along-Scan Pixel.
GDAAC	Goddard DAAC
Granule	A Data Processing Time Unit (5 minutes)
HIRS	High Resolution Infrared Spectrometer
IFOV	Instantaneous Field of View
IR	Infrared
K	Kelvin
L	Radiance
L1B	Level 1B (calibrated, geo-located data)
LUT	Look-Up Table
LWIR	Long Wavelength Infrared
m_1	Reflectance Calibration Linear Term
MCST	MODIS Characterization Support Team
MEM	Main Electronics Module
MODAPS	MODIS Adaptive Processing System
MODIS	Moderate-Resolution Imaging Spectroradiometer
MTPE	Mission To Planet Earth
MWIR	Medium Wavelength Infrared
NASA	National Aeronautics and Space Administration
NIR	Near Infrared
NIST	National Institute of Standards and Technology
nm	Nanometers (10^{-9} meters)
NOAA	National Oceanic and Atmospheric Administration
OBC	On-Board Calibrator
OOB	Out-of-Band
PC	Photoconductive

PFM	Proto-Flight Model (Terra)
PM-1	Post Meridian EOS Platform (Aqua)
PV	Photovoltaic
RSB	Reflective Solar Band (1-19,26)
RSR	Relative Spectral Response
RSS	Root Sum Squared (Uncertainty in the Level 1B Product)
RVS	Response Versus Scan Angle
SAM	Space View Analog Module
SBRS	Santa Barbara Remote Sensing
Scan	1.4771 second cross-track sweep
SD	Solar Diffuser
SDS	Solar Diffuser Screen; also Science Data Set
SDSM	Solar Diffuser Stability Monitor
SDST	Science Data Support Team
SI	Scaled Integer
SiPD	Silicon Photodiode
SIS	Solar Integrating Sphere
SNR	Signal-to-Noise Ratio
SpMA	Spectral Measurement Assembly (used in TV)
SRCA	Spectro-radiometric Calibration Assembly
SV	Space View
SWIR	Short Wavelength Infrared
TBD	To Be Determined
TDI	Time Delay Integration
TEB	Thermal Emissive Band (20-25, 27-36)
Terra	AM-1 satellite that houses MODIS
TM	Thematic Mapper
TOA	Top of the Atmosphere
TV	Thermal Vacuum
UI	Uncertainty Index
VIS	Visible
WUCD	Warm-up, cool-down